DNA double-strand breaks induced by reactive oxygen species promote DNA polymerase IV activity in *Escherichia coli*

Sarah S. Henrikus[1,2], Camille Henry[3], John P. McDonald[4], Yvonne Hellmich[5], Elizabeth A. Wood[3], Roger Woodgate[4], Michael M. Cox[3], Antoine M. van Oijen[1,2], Harshad Ghodke[1,2], Andrew Robinson[1,2]*

[1]Molecular Horizons Institute and School of Chemistry and Biomolecular Science, University of Wollongong, Wollongong, Australia
[2]Illawarra Health and Medical Research Institute, Wollongong, Australia
[3]Department of Biochemistry, University of Wisconsin-Madison, United States of America
[4]Laboratory of Genomic Integrity, National Institute of Child Health and Human Development, National Institutes of Health, Bethesda, Maryland, United States of America
[5]Institute of Biochemistry, Goethe Universität, Frankfurt, Germany

*Corresponding author. Mailing address: School of Chemistry, University of Wollongong, Wollongong, NSW 2500, Australia. Email: andrewr@uow.edu.au.

Under many conditions the killing of bacterial cells by antibiotics is potentiated by DNA damage induced by reactive oxygen species (ROS)[1–3]. A primary cause of ROS-induced cell death is the accumulation of DNA double-strand breaks (DSBs)[1,4–6]. DNA polymerase IV (pol IV), an error-prone DNA polymerase produced at elevated levels in cells experiencing DNA damage, has been implicated both in ROS-dependent killing and in DSBR[7–15]. Here, we show using single-molecule fluorescence microscopy that ROS-induced DSBs promote pol IV activity in two ways. First, exposure to the antibiotics ciprofloxacin and trimethoprim triggers an SOS-mediated increase in intracellular pol IV concentrations that is strongly dependent on both ROS and DSBR. Second, in cells that constitutively express pol IV, treatment with an ROS scavenger dramatically reduces the number of pol IV foci formed upon exposure to antibiotics, indicating a role for pol IV in the repair of ROS-induced DSBs.

Two mechanisms for ROS-induced DSB formation have been proposed (**Figure 1a**). The first invokes oxidisation of the cellular nucleotide pool, leading to increased incorporation of oxidised nucleotide triphosphates (e.g. 8-oxo-dGTP) into the DNA by DNA polymerases[4,7,16]. Subsequent initiation of base-excision repair (BER) creates single-stranded DNA (ssDNA) gaps. In cases where BER is initiated at nearby sites, DSBs may be formed[1,4,7]. Evidence for a second mechanism of ROS-dependent DSB formation has emerged from a recent mechanistic study of thymineless death in *Escherichia coli*[5]. The ROS-driven potentiation of killing by both antibiotic treatment and thymineless death can be abrogated through the addition of ROS scavengers to the culture medium[5,17,18]. Using microscopy to quantify ssDNA gaps and DSBs in cells undergoing thymineless death, Hong and co-workers recently discovered that thymine starvation initially leads to the accumulation of ssDNA gaps, which are subsequently converted to DSBs in an ROS-dependent process[5] (**Figure 1b**). In cells treated with ROS scavengers, gaps are not converted to DSBs and cells are tolerant to thymine starvation[5].

Several lines of evidence implicate pol IV in ROS-dependent DSB formation and/or processing. Pol IV efficiently incorporates 8-oxo-dGTP into DNA *in vitro*[7]. Over-expression of pol IV is lethal to cells and the lethality is ROS-dependent[4,7,19]. Cells lacking pol IV are partially protected against killing by ampicillin under conditions where the nucleotide pool becomes oxidised[7]. These observations are suggestive of pol IV playing a role in the BER-dependent mechanism for DSB formation[4] (**Figure 1a**). Other studies indicate that pol IV has a role in the repair of DSBs[6,9,10,12,13,20–26]. First, pol IV physically interacts with the RecA recombinase; a key player in DSB repair (DSBR)[24]. Second, when expressed from a low-copy plasmid, fluorescently labelled pol IV colocalises with RecA extensively in cells treated with DNA-damaging agents[10]. Pol IV colocalises at sites of induced DSBs in cells[10]. Third, genetic studies reveal that the gene encoding pol IV, *dinB*, is required for both induced and spontaneous error-prone DSBR[6,9,12,13,22,23]. Fourth, intermediates of DSBR known as recombination D-loops are efficiently utilised as substrates by pol IV *in vitro*[25]. Interestingly, pol IV's mutagenic potential is modulated by interaction with the recombinase RecA[20,21,24,26]. Notably, the cellular concentration of pol IV increases significantly upon induction of the SOS response[27,28]. Single-stranded DNA formed during DSBR (through RecBCD-dependent end-resection) is a major trigger for SOS induction under some conditions[29–31].

Here, we used single-molecule fluorescence microscopy to investigate whether ROS, and the DSBs they create, influence pol IV activity in cells. We made use of two antibiotics for which killing is known to involve ROS generation; ciprofloxacin and trimethoprim (**Figure 1a**)[32–35]. For ciprofloxacin, a DNA gyrase inhibitor, a second, ROS-independent pathway exists in which gyrase-stabilised cleavage complexes dissociate, creating a DSB (**Figure**

1b)[32,33,36,37]. During antibiotic treatment, we would expect that some pol IV binding would be dependent on ROS and/or DSB processing while others would be independent of these factors. Throughout the study, we used dimethyl sulfoxide (DMSO) to create low ROS conditions. DMSO is an effective scavenger of antibiotic-induced ROS[5,38]. In agreement with the scheme in **Figure 1a**, co-treatment with DMSO increases survival in cells exposed to both ciprofloxacin and trimethoprim[5,38] (**Supplementary figure 1,2**).

To compare pol IV behaviour under high-ROS (no DMSO) and low-ROS (DMSO added) conditions, we recorded time-lapse movies (180 min duration)[28,39] of cells treated with i) ciprofloxacin alone, ii) ciprofloxacin and DMSO in combination, iii) trimethoprim alone or iv) trimethoprim and DMSO in combination (**Figure 2**). Following antibiotic addition, we recorded time-lapse movies capturing fluorescence from a functional DinB-YPet fusion[28]. Cells treated with ciprofloxacin became filamentous and showed a clear increase in DinB-YPet intensity (**Figure 2a,b; Supplementary figure 3**). This is consistent with our previous study in which we measured a six-fold increase in intracellular DinB-YPet (pol IV) concentrations from 6 ± 1 nM prior to treatment to 34 ± 3 nM 180 min after ciprofloxacin addition[28]. Interestingly, inclusion of the ROS scavenger DMSO led to a significant reduction in ciprofloxacin-induced up-regulation of pol IV levels; 180 min after ciprofloxacin addition, cellular DinB-YPet intensities were increased above basal levels by less than 3 fold (**Figure 2a,b**), corresponding to a final concentration of ~17 nM (see **Materials and Methods**). Treatment with trimethoprim alone led to a significant increase in DinB-YPet fluorescence; 180 min after trimethoprim addition the mean fluorescence intensity increased by 50% of ciprofloxacin-alone levels (**Figure 2a,b**), corresponding to a final intracellular pol IV concentration of ~20 nM. Inclusion of DMSO led to a significant reduction in trimethoprim-induced up-regulation; cell-associated DinB-YPet intensities increased by only 11% compared with ciprofloxacin-alone treatment, corresponding to a final pol IV concentration of ~9 nM. Thus, for both the ciprofloxacin and trimethoprim treatments, addition of the ROS scavenger DMSO significantly reduces the up-regulation of pol IV in response to antibiotic treatment.

Ciprofloxacin-treated cells also produced multiple DinB-YPet foci (**Figure 2c**). These foci require the catalytic activity of pol IV and are produced as individual DinB-YPet molecules bind to DNA and thus experience decreased diffusional mobility[28], a phenomenon known as detection by localisation[40]. Prior to the addition of ciprofloxacin, cells contained on average 0.6 ± 0.2 foci per cell in the absence of DMSO, and 0.4 ± 0.1 foci per cell in the presence of DMSO (**Figure 2c**). Following treatment with ciprofloxacin alone, the number of foci steadily increased. By 180 min, cells had 4.2 ± 1.1 foci per cell. Upon ciprofloxacin-DMSO treatment, cells contained 1.8 ± 0.4 foci per cell; a significant reduction compared to ciprofloxacin-alone measurements. Addition of DMSO reduced the number of DinB-YPet foci by >50%. Prior to the addition of trimethoprim, cells contained on average 0.5 ± 0.1 foci in the absence of DMSO and 0.4 ± 0.1 foci in the presence of DMSO. Trimethoprim-alone treatment induced a slight increase in the number of DinB-YPet foci with 0.9 ± 0.2 per cell at 180 min. This is lower than the number of foci observed for ciprofloxacin-DMSO treatment (1.8 ± 0.4 per cell), despite the measured pol IV concentration being marginally higher after trimethoprim-alone treatment (**Figure 2b**). Strikingly, cells treated with both trimethoprim and DMSO did not show any increase in DinB-YPet foci after trimethoprim addition (0.5 ± 0.1 foci per cell at 180 min; **Figure 2c**). Together, these studies demonstrate that treatment with DMSO in addition to either ciprofloxacin or trimethoprim treatment not only supresses the SOS-induced up-regulation of DinB-YPet, but also the binding of DinB-YPet to its cellular substrates.

Reasoning that the decreased induction of DinB-YPet expression in cells co-treated with DMSO likely resulted from attenuation of the SOS response, we repeated the time-lapse experiments on cells that carried an SOS-reporter plasmid, in which GFP is expressed from the SOS-inducible *sulA* promoter (pUA66 P*sulA*-GFP; fast-folding GFP, *gfpmut2*[41]). In the absence of any antibiotic treatments, cells exhibit very low fluorescence intensity, consistent with the repression of the *sulA* promoter in the absence of exogenous sources of DNA damage (**Figure 3,** '0 min'). SOS levels were similarly low for cells grown in the presence of DMSO. Cells exhibited robust SOS induction upon treatment with ciprofloxacin as evidenced by the increase in GFP fluorescence in the three hour time window after addition of ciprofloxacin (**Figure 3b**). Consistent with our hypothesis, SOS induction was strongly inhibited upon inclusion of DMSO during ciprofloxacin treatment (7% of ciprofloxacin-alone levels at 180 min; **Figure 3b**). Similarly, high levels of SOS induction in trimethoprim treated cells were supressed by the addition of DMSO (0.6% of ciprofloxacin-alone levels; **Figure 3b**). Notably, the addition of a different ROS scavenger, 2,2'-bipyridine (BiP, 0.35 mM, 0.5 x MIC[5]), similarly supressed the induction of the SOS response (**Figure 3**).

We further reasoned that the suppression of SOS by ROS scavengers might reflect a reduction in the formation and processing of DSBs. It was previously observed that induction of SOS by the antibiotic nalidixic acid was completely blocked in cells that carried a *recB* mutation and were therefore incapable of processing DSBs through the RecBCD end-resection nuclease complex[30,31]. This implies that SOS is primarily triggered by DSB processing in nalidixic acid-treated cells. As ciprofloxacin and nalidixic acid both target DNA gyrase[32,33,42], we repeated the GFP reporter measurements in cells lacking *recB* (SSH111, Δ*recB* P*sulA*-GFP) to determine if SOS induction by ciprofloxacin is also dependent on DSB processing. The deletion of *recB* strongly inhibited the SOS response following ciprofloxacin treatment (~0.4% induction at 180 min in comparison to *recB*$^+$, **Figure 3, Supplementary figure 4**). While *recB* deletions are known to reduce survival in cells treated with ciprofloxacin[43], we observed that most cells lacking *recB* continued to grow and divide during the 180 min time-lapse measurement (**Supplementary figure 3,4**), indicating that the lack of SOS induction observed for ciprofloxacin-treated *recB*-deficient cells did not stem from gross inhibition of all cellular functions. Thus, induction of the SOS response is dependent on DSB processing in cells treated with ciprofloxacin. Together the results are consistent with a model in which the SOS response is triggered in antibiotic-treated cells via ROS-induced DSBs, leading to increased levels of pol IV in cells.

We next considered the possibility that pol IV plays a direct role in DSBR. To this end we examined rates of DinB-YPet focus formation in cells treated with ciprofloxacin and trimethoprim, comparing conditions that permitted DSB resection (*recB*$^+$, no DMSO) or prevented DSB resection (co-treatment with DMSO to supress ROS-induced DSB formation, or Δ*recB* to prevent resection). To separate effects on focus formation from effects on DinB-YPet expression, these measurements were carried out in a *lexA*(Def) background[44] (*dinB-YPet dnaX-mKate2 lexA*[Def]). These cells constitutively express DinB-YPet at levels consistent with SOS induced levels, even in the absence of DNA damage[28]. Consistent with the results from our previous study[28], close to zero DinB-YPet foci were observed in *lexA*(Def) cells in the absence of antibiotic (0.08 ± 0.05 foci per cell, **Figure 4**). *lexA*(Def) cells treated with ciprofloxacin for 60 min exhibited clear foci (1.43 ± 0.15 foci per cell, **Figure 4b**). Co-treatment with ciprofloxacin and DMSO yielded fewer foci (1.02 ± 0.13 foci per cell, **Figure 4b**). In Δ*recB*, cells contained 0.23 ± 0.05 foci per cell. Cells treated with trimethoprim for 60 min contained DinB-YPet foci (2.6 ± 0.18 foci per cell), whereas cells

treated with both trimethoprim and DMSO contained few foci (0.19 ± 0.06). Trimethoprim-treated Δ*recB* cells also contained very few foci (0.14 ± 0.05). Similar effects were observed in *lexA*$^+$ cells, although reductions in focus formation were conflated with reductions in DinB-YPet expression levels (**Figure 2c**). Together, these results indicate that reducing the number of ROS-induced DSBs being formed, and inhibiting DSB resection, upon antibiotic treatment led to reduced focus formation by DinB-YPet. This implies that pol IV is normally active at ROS-induced DSBs in cells treated with ciprofloxacin or trimethoprim. Importantly, RecBCD function is critical for pol IV activity.

In ciprofloxacin-treated cells, 10% of pol IV foci form in the vicinity of replisomes[28]. Here we observed that in addition to reducing the number of DinB-YPet foci, DMSO treatment dramatically increased the relative colocalisation of DinB-YPet with replisomes in both *lexA*$^+$ and *lexA*(Def) cells treated with ciprofloxacin (**Supplementary figure 5, 6**). For long-lived pol IV foci (detectable within a 10s average projection image) in the *lexA*(Def) background, 80% of foci colocalised with replisomes under ciprofloxacin-DMSO conditions (**Supplementary figure 6b**). This is consistent with the addition of DMSO having removed the vast majority of non-replisomal substrates for pol IV-dependent DNA synthesis. For *lexA*(Def) cells treated with trimethoprim, addition of DMSO abolished long-lived pol IV foci entirely (**Supplementary figure 6a,c**).

Finally, we explored if ROS-induced DSBs promote a change in the binding activity of the other major error-prone polymerase in *E. coli*, pol V (UmuD'$_2$C). As before, a *lexA*(Def) background (RW1286, *umuC-mKate2 dnaX-YPet lexA*[Def]) was used to separate effects on focus formation from effects on UmuC-mKate2 expression. Few UmuC-mKate2 foci were observed in the absence of antibiotic (about 0.32 ± 0.08 foci per cell, **Supplementary figure 7**). In cells treated with ciprofloxacin or trimethoprim for 60 min, foci were clearly visible (ciprofloxacin: 1.24 ± 0.16 foci per cell; trimethoprim 1.39 ± 0.21 foci per cell). In both cases, co-treatment with DMSO had little effect on the number of UmuC-mKate2 foci (ciprofloxacin-DMSO: 0.99 ± 0.12 foci per cell; trimethoprim-DMSO 1.26 ± 0.16 foci per cell) or the overall levels of UmuC-mKate2 fluorescence in the cells. Thus in contrast to the effects observed for pol IV, ROS-induced DSBs had little effect on pol V activity. Interestingly, trimethoprim treatment (with or without DMSO) did not lead to activation of pol V: UmuC-mKate2 failed to undergo its characteristic spatial redistribution[39], remaining bound to the cell membrane (**Supplementary figure 8a, c**). Consistent with this, cleavage of UmuD to UmuD′ was far less efficient in trimethoprim-treated cells than in ciprofloxacin-treated cells (compare **Supplementary figure 9b** and **d**).

We conclude that the processing of ROS-induced DSBs induces high intracellular concentrations of DinB-YPet and promotes focus formation. The observations are consistent with a model in which ROS-induced DSBs promote pol IV activity by inducing the SOS response and by generating substrates for pol IV in the form of recombination intermediates. Few DinB-YPet foci were observed in cells treated with a combination of trimethoprim and DMSO (**Figure 4**). Based on events that occur during the analogous process of thymineless death[5,45], treatment with trimethoprim should induce the formation of ssDNA gaps in the wake of the replisome. In the presence of ROS these would be rapidly converted to DSBs, whereas in the presence of ROS scavengers the gaps would persist. The low extent of focus formation observed under trimethoprim-DMSO conditions implies that pol IV rarely acts at these ssDNA gaps. In contrast, the formation of foci by the pol V was not affected by the addition of DMSO (**Supplementary figure 7**). This implies that ssDNA gaps might represent a major substrate for pol V and that DSB intermediates are rarely acted upon by pol V. In cells treated with ciprofloxacin, the colocalisation of DinB-YPet with replisomes was

substantially increased in the presence of DMSO. Ciprofloxacin induces the formation of end-stabilised DNA-gyrase complexes, which slow cell growth but are non-lethal[46]. It is possible that replisome-proximal DinB-YPet foci, that are insensitive to ROS, reflect pol IV molecules that are recruited to replisomes that have stalled at end-stabilised DNA-gyrase complexes.

Methods

Strain construction

EAW102 is *E. coli* K-12 MG1655 Δ*recB* and was constructed using λ_{RED} recombination. The kanamycin resistance marker in EAW102 was removed via FLP-FRT recombination[47] using the plasmid pLH29 to obtain kanamycin sensitive HG356.

SSH091 and SSH111 (*dinB*$^+$ *lexA*$^+$ *recB*$^+$ + pUA66-*sulA*-GFP and *dinB*$^+$ *lexA*$^+$ Δ*recB::FRT* + pUA66-*sulA*-GFP) were created by transforming MG1655 and EAW102 with pUA66-*sulA*-GFP[41].

RW1286 is *E. coli* MG1655 *umuC-mKate2 dnaX-YPet sulA*$^-$::kan^R *lexA51*(Def)::Cm^R and was made in two steps: first the wild-type *sulA*+ gene of EAW282 was replaced with *sulA*$^-$::kan by P1 transduction from EAW13[39], to create EAW282 *sulA*$^-$; then *lexA51*(Def) *malB*::Tn*9* was transferred from DE406[44] into EAW282 *sulA*$^-$ by P1 transduction, selecting for chloramphenicol resistance. To confirm the presence of the *lexA*(Def) genotype, colonies were then screened for high levels of RecA expression by Western blotting with anti-RecA antibodies[48].

EAW1144 is *E. coli* K-12 MG1655 *dinB-YPet dnaX-mKate2 sulA*$^-$ *lexA51*(Def) Δ*recB* and was constructed in three steps: *sulA*$^-$ FRT-Kan-FRT was P1 transduced in EAW643 (KanS) using a P1 lysate grown on EAW13 to obtain the strain EAW1134. The Kan cassette was removed using pLH29[47]. Then, *lexA51*(Def) *malB*::Tn*9* was transduced into EAW1134 using a P1 lysate grown on DE406 to obtain the strain EAW1141. Finally, Δ*recB* FRT-KanR-FRT was transduced into EAW1141using P1 lysate grown on EAW102 to obtain EAW1144. All mutations introduced were confirmed by PCR.

Table 1. Strains used in this study.

Strain	Relevant Genotype	Parent strain	Source/technique
MG1655	*dinB*$^+$ *dnaX*$^+$ *recB*$^+$ *lexA*$^+$	-	published[49]
EAW102	Δ*recB*::Kan^R	MG1655	Lambda Red recombination
HG356	Δ*recB*::FRT	MG1655	EAW102
SSH091	*dinB*$^+$ *lexA*$^+$ *recB*$^+$ + pUA66-*sulA*-GFP	MG1655	Transformation of MG1655 with pUA66-*sulA*-GFP
SSH111	*dinB*$^+$ *lexA*$^+$ Δ*recB*::FRT + pUA66-*sulA*-GFP	HG356	Transformation of HG356 with pUA66-*sulA*-GFP[41]
EAW18	Δ*dinB*::Kan^R	MG1655	published[28]
RW120	*recA*$^+$ *sulA*$^-$	RW118	published[50]

	lexA$^+$ Δ*umuDC*::Cm^R		
RW546	*recA*+ *sulA*$^-$ *lexA51*(Def) Δ*umuDC*::Cm^R	RW542	published[51]
RW880	Δ*umuDC*::Cm^R	MG1655	Transduction of MG1655 with P1 grown on RW120[50]
JJC5945	*dnaX-YPet*::Kan^R	MG1655	published[39]
EAW642	*dnaX-mKate2*::Kan^R	MG1655	published[28]
EAW633	*dinB-YPet*::Kan^R	MG1655	published[28]
EAW643	*dinB-YPet*::FRT *dnaX-mKate2*::Kan^R	EAW633	published[28]
EAW191	*umuC-mKate2*::Kan^R	MG1655	published[39]
EAW282	*umuC-mKate2*::FRT *dnaX-YPet*::Kan^R	JJC5945	published[39]
EAW13	*sulA*$^-$::Kan^R	MG1655	published[39]
EAW282 *sulA*$^-$	*umuC-mKate2*::FRT *dnaX-YPet*::FRT *sulA*$^-$::Kan^R	EAW282	Transduction of EAW282 with P1 grown on EAW13
RW1286	*umuC-mKate2*::FRT *dnaX-YPet*::FRT *sulA*$^-$::Kan^R *lexA51*(Def)::Cm^R	EAW282 *sulA*$^-$	Transduction of EAW282 *sulA*$^-$ with P1 grown on DE406[44]
RW1594	*dinB-YPet dnaX-mKate2 sulA*$^-$::Kan^R *lexA51*(Def)::Cm^R	RW1588	published[28]
EAW1134	*dinB-YPet*::FRT *dnaX-mKate2*::FRT *sulA*$^-$::Kan^R	EAW643	Transduction of EAW643 with P1 grown on EAW13
EAW1141	*dinB-YPet*::FRT *dnaX-mKate2*::FRT *sulA*$^-$::FRT *lexA51*(Def)::Cm^R	EAW1134	Transduction of EAW1134 with P1 grown on DE406
EAW1144	*dinB-YPet*::FRT *dnaX-mKate2*::FRT *sulA*$^-$::FRT *lexA51*(Def)::Cm^R Δ*recB*::Kan^R	EAW1141	Transduction of EAW1141 with P1 grown on EAW102

DNA damaging agent sensitivity assay

Cells were grown in LB overnight at 37ºC. The next day, a 1/100 dilution of each culture was grown in LB medium (at 37ºC, 150 rpm) until reaching mid log phase (OD_{600} = 0.2). Cell cultures were then serially diluted in PBS by factors of ten down to 10^{-5}. Serial dilutions were spotted (spot volume 10 µL) on fresh LB plates (Difco brand) and LB plates containing DNA damaging agent (which were protected from light). For Supplementary figure 1, DNA damaging agents were added at the following concentrations: 0.1 µg/mL trimethoprim; 12 ng/mL ciprofloxacin. For Supplementary figure 2, DNA damaging agents were added at the following concentrations: 0.1 µg/mL or 0.2 µg/mL trimethoprim; 10 ng/mL or 12 ng/mL ciprofloxacin. Some survival essays were performed under radical-scavenging conditions. Additionally to the particular antibiotic, DMSO (2% v/v, 282 mM, 0.2 x MIC[5]) was then also added to the plates. Plates were incubated at 37ºC in the dark.

Trimethoprim survival assay

Cells were grown in LB overnight at 37^0C. The next day, a 1/100 dilution of each culture was grown in 5 mL LB medium (at 37^0C, 150 rpm) until reaching mid log phase (OD_{600} = 0.3). Then, trimethoprim was added to 1 µg/mL followed by incubation at 37^0C, 150 rpm. Samples of 500 µL were taken at 0, 0.5, 1, 2, 3 and 5 h; samples at 0h were taken just before trimethoprim addition. Each sample was centrifuged and resuspended in 500 µL LB; this was done twice to dilute out trimethoprim. Then, 50 µL of 500 µL were plated on LB agar plates; three technical replicates were made for each time point and strain. Plates were incubated at 37^0C in the dark. The next day, colonies were counted and CFU/mL were calculated for each time point; the average over the technical replicates was then calculated. Two biological replicates were performed. Data points represent the average over the biological duplicates. Error bars represent standard error of the mean over two biological replicates.

Fluorescence microscopy

Wide-field fluorescence imaging was conducted on an inverted microscope (IX-81, Olympus with a 1.49 NA 100x objective) in an epifluorescence configuration. Continuous excitation is provided using semidiode lasers (Sapphire LP, Coherent) of the wavelength 514 nm (150 mW max. output) and 568 nm (200 mW max. output). DnaX-mKate2 in EAW643 and UmuC-mKate2 in EAW282 were imaged using yellow excitation light (λ = 568 nm) at high intensity (2750 Wcm^{-2}), collecting emitted light between 610–680 nm (ET 645/75m filter, Chroma) on a 512 × 512 pixel EM-CCD camera (C9100-13, Hamamatsu). Images of UmuC-mKate2 in RW1286 were recorded at 275 Wcm^{-2}. For DinB-YPet imaging of EAW643, we used green excitation (λ = 514 nm) at 160 Wcm^{-2} collecting light emitted between 525–555 nm (ET540/30m filter, Chroma). For DinB-YPet imaging of RW1594, cells were imaged at 51 Wcm^{-2}. DnaX-YPet imaging (EAW282, RW1286) was performed at 51 Wcm^{-2}. Cells carrying the SOS reporter plasmid pUA66-*sulA*-GFP (SSH091, SSH111) were imaged at 16 Wcm^{-2}.

Two-colour time-lapse movies were recorded to visualise if DinB-YPet foci overlap with DnaX-mKate2 foci (EAW643). Sets of three images were recorded (bright-field [34 ms exposure], mKate2 fluorescence [100 ms exposure], YPet fluorescence [50 ms exposure]) at an interval of 10 min for 3h. To measure colocalisation between UmuC-mKate2 with the replisome marker DnaX-YPet (EAW282), we recorded time-lapse movies at the same intervals but different exposures for the replisome marker (bright-field [34 ms exposure], mKate2 fluorescence [100 ms exposure], YPet fluorescence [500 ms exposure]).

Burst acquisitions of DinB-YPet (movies of 300 × 50 ms frames taken every 100 ms light at 514 nm) were collected, subsequently to each burst acquisition, an image of DnaX-mKate2 (568 nm) was taken (imaging sequence for RW1594). With this imaging sequence, we analysed activity of DinB-YPet at replisomes. RW1286 was imaged similarly; we recorded burst acquisitions of UmuC-mKate2 (568 nm) followed by a snapshot of DnaX-YPet (514 nm). All images were analysed with ImageJ[52].

Flow cell designs

All imaging experiments were carried out in home-built quartz-based flow cells. These flow cells were assembled from a no. 1.5 coverslip (Marienfeld, REF 0102222), a quartz top piece (45x20x1 mm) and PE-60 tubing (Instech Laboratories, Inc.). Prior to flow-cell assembly, coverslips were silanised with (3-aminopropyl)triethoxysilane (Alfa Aeser). First, coverslips were sonicated for 30 min in a 5M KOH solution to clean and activate the

surface. The cleaned coverslips were rinsed thoroughly with MilliQ water and then treated with a 5% (v/v) solution of (3-aminopropyl)triethoxysilane (APTES) in MilliQ water. The coverslips were subsequently rinsed with ethanol and sonicated in ethanol for 20 seconds. Afterwards, the coverslips were rinsed with MilliQ water and dried in a jet of N_2. Silanised slides were stored under vacuum prior to use.

To assemble each flow cell, polyethylene tubing (BTPE-60, Instech Laboratories, Inc.) was glued (BONDiT B-482, Reltek LLC) into two holes that were drilled into a quartz piece. After the glue solidified overnight, double-sided adhesive tape was stuck on two opposite sides of the quartz piece to create a channel. Then, the quartz piece was stuck to an APTES-treated coverslip. The edges were sealed with epoxy glue (5 Minute Epoxy, PARFIX). Each flow cell was stored in a desiccator under mild vacuum while the glue dried. Typical channel dimensions were 45 mm × 5 mm × 0.1 mm (length × width × height).

Imaging in flow cells

For all imaging experiments, cells were grown at 37^0C in EZ rich defined medium (Teknova) that contained 0.2% (w/v) glucose. All strains that have a *Kan*^{R} cassette were grown in the presence of kanamycin (20 µg/mL). Cultures used for imaging under radical-scavenging conditions were grown in the presence of the particular scavenger used for the experiment (DMSO [2% v/v, 282 mM, 0.2 x MIC[5]] or BiP [0.35 mM, 0.5 x MIC[5]], culture time ~3h).

Cells were loaded into flow cells, allowed a few minutes to associate with the APTES surface, then loosely associated cells were removed by pulling through fresh medium. The experiment was then initiated by adding either an antibiotic alone or in combination with DMSO to the medium (30 ng/ mL ciprofloxacin, 30 ng/ mL ciprofloxacin with 2% (v/v) DMSO, 1 µg/mL trimethoprim, 1 µg/mL trimethoprim with 2% (v/v) DMSO or 1 µg/mL trimethoprim with 0.35 mM BiP). Throughout the experiment, medium was pulled through the flow cell using a syringe pump, at a rate of 50 µL/min. For each condition, triplicate measurements were recorded.

Analysis of cell filamentation, concentrations, SOS induction level and number of foci

We selected single cells to obtain information about SOS induction, DinB and UmuC levels upon UV irradiation (>100 cells for every time point). MicrobeTracker 0.937[53], a MATLAB script, was used to create cell outlines as regions of interest (ROI). We manually curated cell outlines designated by MicrobeTracker at t = 0 min (time point of antibiotic addition) and at 30 min time intervals until 180 min. By obtaining cell outlines manually, we ensure accuracy and purely select non-overlapping, in-focus cells for analysis. These ROI were imported in ImageJ 1.50i. The cell outlines were then used to measure mean cell intensities, cell lengths and the number of foci per cell. Parameters describing foci (number, positions and intensities) were obtained using a Peak Fitter plug-in, described previously [28,39].

Analysis of colocalisation events

Foci were classed as colocalised if their centroid positions (determined using our peak fitter tool) fell within 2.18 px (218 nm) of each other. When treating with ciprofloxacin, we determined that for DinB-YPet–DnaX-mKate2 localisation the background of DinB foci expected to colocalise with replisomes purely by chance is ~4% at 180 min. This was calculated by taking the area of each cell occupied by replisome foci (including the colocalisation search radius) and dividing by the total area of the cell. The value of 4% corresponds to the mean of measurements made over 121 cells. Since the foci density of

replisomes stays fairly constant following ciprofloxacin treatment, the chance colocalisation of DinB-YPet foci with DnaX-mKate2 is ~4% during the experiment[28]. Chance colocalisation of DnaX-mKate2 with DinB-YPet is however not constant over time because most cells contain no pol IV foci in the absence of any DNA damage. Chance colocalisation is close to zero at 0 min; at 60 min, chance colocalisation is ~5%; at 120 min, chance colocalisation is ~3%. Moreover, chance colocalisation of DnaX-mKate2 with DinB-YPet is overall reduced under radical-scavenging conditions due to a reduced number of foci per cell (chance colocalisation close to zero at 0 min; at 120 min, ~2%). Chance colocalisation of DnaX-mKate2 with DinB-YPet in trimethoprim treated cells amounts to ~1% from 60-90 min (close to zero before 60 min). Under radical-scavenging conditions, chance colocalisation is always close to zero because the number of pol IV foci per cell does not increase post treatment as well as cell size (**Figure 2**).

The chance colocalisation of UmuC-mKate2 with DnaX-YPet is similar to the chance colocalisation of DinB-YPet with DnaX-mKate2 (chance colocalisation: ~4%). The expected colocalisation of DnaX-YPet with UmuC-mKate2 by background is close to zero until 90 min. UmuC-mKate2 is neither upregulated nor released from the membrane (**Supplementary figure 8a**). Chance colocalisation is ~3% at 180 min after ciprofloxacin treatment and ~2% after the combinational treatment of ciprofloxacin/DMSO.

Western blotting

Overnight *E. coli* LB cultures of RW120/pRW154 and RW546/pRW154[50] were diluted 1 to 100 in fresh LB with appropriate antibiotics and grown to mid-log (~OD 0.5, ~3 hrs). Aliquots were then taken for the untreated samples. Either ciprofloxacin (30 ng/mL) or trimethoprim (1 µg/mL) was added to the remaining culture and incubated with or without the addition of 2% DMSO. Samples were taken at 1, 2 and 3 hours. Whole cell extracts were made by centrifuging 1.5 mL of culture and adding 90 µl of sterile deionized water and 30µL of NuPAGE LDS sample buffer (4X) (Novex, Life Technologies) to the cell pellet. Five cycles of freeze/thaw on dry ice and in a 37^0C water bath were performed to lyse the cells. Extracts were boiled for 5 minutes prior to loading. Samples were run on NuPAGE 4-12% Bis-Tris gels (Novex Life Technologies) and transferred to Invitrolon PVDF (0.45 µm pore size) membranes (Novex Life Technologies). Membranes were incubated with anti-UmuD antibodies (1:5,000 dilution) at room temperature overnight. Then the membranes were incubated with goat anti-rabbit IgG (H+L) alkaline phosphatase conjugate (1:10,000 dilution) (BIO-RAD). Subsequently, the membranes were treated with the CDP-Star substrate (Tropix). Membranes were then exposed to BioMax XAR film (Carestream) to visualise UmuD protein bands.

References

1. Dwyer, D. J., Collins, J. J. & Walker, G. C. Unraveling the physiological complexities of antibiotic lethality. *Annu. Rev. Pharmacol. Toxicol.* **55,** 313–332 (2015).

2. van Acker, H. & Coenye, T. The role of reactive oxygen species in antibiotic-mediated killing of bacteria. *Trends Microbiol.* **25,** 456–466 (2017).

3. Dwyer, D. J., Kohanski, M. A. & Collins, J. J. Role of reactive oxygen species in mechanisms of antimicrobial resistance in bacteria. *Curr. Opin. Microbiol.* **12,** 482–489 (2009).

4. Gruber, C. C. & Walker, G. C. Incomplete base excision repair contributes to cell death from antibiotics and other stresses. *DNA Repair.* **71,** 108–117 (2018).

5. Hong, Y., Li, L., Luan, G., Drlica, K. & Zhao, X. Contribution of reactive oxygen species to thymineless death in *Escherichia coli*. *Nat. Microbiol.* **2,** 1667–1675 (2017).

6. Moore, J. M., Correa, R., Rosenberg, S. M. & Hastings, P. J. Persistent damaged bases in DNA allow mutagenic break repair in *Escherichia coli*. *PLoS Genet.* **13,** e1006733 (2017).

7. Foti, J. J., Devadoss, B., Winkler, J. A., Collins, J. J. & Walker, G. C. Oxidation of the guinine nucleotide pool underlies cell death by bactericidial antibiotics. *Science.* **336,** 315–319 (2012).

8. Sekiguchi, M. & Tsuzuki, T. Oxidative nucleotide damage: Consequences and prevention. *Oncogene* **21,** 8895–8904 (2002).

9. Ponder, R. G., Fonville, N. C. & Rosenberg, S. M. A switch from high-fidelity to error-prone DNA double-strand break repair underlies stress-induced mutation. *Mol. Cell* **19,** 791–804 (2005).

10. Mallik, S., Popodi, E. M., Hanson, A. J. & Foster, P. L. Interactions and localization of *Escherichia coli* error-prone DNA polymerase IV after DNA damage. *J. Bacteriol.* **197,** 2792–2809 (2015).

11. Motamedi, M. R., Szigety, S. K. & Rosenberg, S. M. Double-strand-break repair recombination in *Escherichia coli*: physical evidence for a DNA replication mechanisms *in vivo*. *Genes Dev.* **13,** 2889–2903 (1999).

12. Shee, C., Gibson, J. L., Darrow, M. C., Gonzalez, C. & Rosenberg, S. M. Impact of a stress-inducible switch to mutagenic repair of DNA breaks on mutation in *Escherichia coli*. *Proc. Natl. Acad. Sci. U. S. A.* **108,** 13659–13664 (2011).

13. Rosenberg, S. M., Shee, C., Frisch, R. L. & Hastings, P. J. Stress-induced mutation via DNA breaks in *Escherichia coli*: A molecular mechanism with implications for evolution and medicine. *Bioessays* **34,** 885–892 (2012).

14. Shee, C., Gibson, J. L. & Rosenberg, S. M. Two mechanisms produce mutation hotspots at DNA breaks in *Escherichia coli*. *Cell Rep.* **2,** 714–721 (2012).

15. Frisch, R. L. *et al.* Separate DNA Pol II- and Pol IV-dependent pathways of stress-induced mutation during double-strand-break repair in *Escherichia coli* are controlled by RpoS. *J. Bacteriol.* **192,** 4694–4700 (2010).

16. Giroux, X., Su, W.-L., Bredeche, M.-F. & Matic, I. Maladaptive DNA repair is the ultimate contributor to the death of trimethoprim-treated cells under aerobic and anaerobic conditions. *Proc. Natl. Acad. Sci. U. S. A.* **114,** 11512–11517 (2017).

17. Zhao, X. & Drlica, K. Reactive oxygen species and the bacterial response to lethal stress. *Curr. Opin. Microbiol.* **21,** 1–6 (2014).

18. Kaur, P. *et al.* Involvement of reactive oxygen species in the action of ciprofloxacin against *Escherichia coli*. *Future Microbiol.* **6,** 949–954 (2014).

19. Yamada, M. *et al.* Involvement of Y-family DNA polymerases in mutagenesis caused by oxidized nucleotides in *Escherichia coli*. *J. Bacteriol.* **188,** 4992–4995 (2006).

20. Indiani, C., Patel, M., Goodman, M. F. & O'Donnell, M. E. RecA acts as a switch to

regulate polymerase occupancy in a moving replication fork. *Proc. Natl. Acad. Sci. U. S. A.* **110,** 5410–5415 (2013).

21. Cafarelli, T. M., Rands, T. J. & Godoy, V. G. The DinB·RecA complex of *Escherichia coli* mediates an efficient and high-fidelity response to ubiquitous alkylation lesions. *Environ. Mol. Mutagen. Mutagen.* **55,** 92–102 (2014).

22. Shee, C., Ponder, R., Gibson, J. L. & Rosenberg, S. M. What limits the efficiency of double-strand break-dependent stress-induced mutation in *Escherichia coli*? *J. Mol. Microbiol. Biotechnol.* **21,** 8–19 (2012).

23. Foster, P. L. Stress-induced mutagenesis in bacteria. *Crit. Rev. Biochem. Mol. Biol.* **42,** 373–397 (2007).

24. Godoy, V. G., Jarosz, D. F., Simon, S. M., Abyzov, A. & Walker, G. C. UmuD and RecA directly modulate the mutagenic potential of the Y-family DNA polymerase DinB. *Mol. Cell* **28,** 1058–1070 (2007).

25. Pomerantz, R. T., Kurth, I., Goodman, M. F. & O'Donnell, M. Preferential D-loop extension by a translesion DNA polymerase underlies error-prone recombination. *Nat. Struct. Mol. Biol.* **20,** 748–755 (2013).

26. Pomerantz, R. T., Goodman, M. F. & O'Donnell, M. E. DNA polymerases are error-prone at RecA-mediated recombination intermediates. *Cell Cycle* **12,** 2558–2563 (2013).

27. Courcelle, J., Khodursky, A., Peter, B., Brown, P. O. & Hanawalt, P. C. Comparative gene expression profiles following UV exposure in wild-type and SOS-deficient. *Genetics* **158,** 41–64 (2001).

28. Henrikus, S. S. *et al.* DNA polymerase IV primarily operates outside of DNA replication forks in *Escherichia coli*. *PLoS Genet.* **14,** e1007161 (2018).

29. Vlašić, I., Ivančić-Baće, I., Imešek, M., Mihaljević, B. & Brčić-Kostić, K. RecJ nuclease is required for SOS induction after introduction of a double-strand break in a RecA loading deficient *recB* mutant of *Escherichia coli*. *Biochimie* **90,** 1347–1355 (2008).

30. McPartland, A., Green, L. & Echols, H. Control of *recA* gene RNA in *E. coli*: Regulatory and signal genes. *Cell* **20,** 731–737 (1980).

31. Newmark, K. G., O'Reilley, E. K., Pohlhaus, J. R. & Kreuzer, K. N. Genetic analysis of the requirements for SOS indcution by nalidixic acid in *Escherichia coli*. *Gene* **356,** 69–76 (2005).

32. Zhao, X., Xu, C., Domagala, J. & Drlica, K. DNA topoisomerase targets of the fluoroquinolones: a strategy for avoiding bacterial resistance. *Proc. Natl. Acad. Sci. U. S. A.* **94,** 13991–13996 (1997).

33. Drlica, K. & Zhao, X. DNA gyrase, topoisomerase IV, and the 4-quinolones. *Microbiol. Mol. Biol. Rev.* **61,** 377–392 (1997).

34. Birdsall, B., Roberts, G. C., Feeney, J., Dann, J. & Burgen, A. Trimethoprim binding to bacterial and mammalian dihydrofolate reductase: a comparison by proton and carbon-13 nuclear magnetic resonance. *Biochemistry* **22,** 5597–5604 (1983).

35. Zheng, Q., Jockusch, S., Zhou, Z. & Blanchard, S. C. The contribution of reactive oxygen species to the photobleaching of organic fluorophores. *Photochem. Photobiol.* **90,** 448–454 (2014).

36. Champoux, J. J. DNA topoisomerases: structure, function, and mechanism. *Annu. Rev. Biochem.* **70,** 369–413 (2001).

37. Drlica, K., Malik, M., Kerns, R. J. & Zhao, X. Quinolone-mediated bacterial death. *Antimicrob. Agents Chemother.* **52,** 385–392 (2008).

38. Mi, H. *et al.* Dimethyl sulfoxide protects *Escherichia coli* from rapid antimicrobial-mediated killing. *Antimicrob. Agents Chemother.* **60,** 5054–5058 (2016).

39. Robinson, A. *et al.* Regulation of mutagenic DNA polymerase V activation in space and time. *PLoS Genet.* **11,** e1005482 (2015).

40. Li, G.-W. & X. Sunney Xie. Central dogma at the single-molecule level of living cells. *Nature* **475,** 308–315 (2011).

41. Zaslaver, A. *et al.* A comprehensive library of fluorescent transcriptional reporters for *Escherichia coli*. *Nat. Methods* **3,** 623–628 (2006).

42. Shen, L. L. & Pernet, A. G. Mechanism of inhibition of DNA gyrase by analogues of nalidixic acid: The target of the drugs is DNA. *Proc. Natl. Acad. Sci. U. S. A.* **82,** 307–311 (1985).

43. Dorr, T., Lewis, K. & Vulic, M. SOS response induces persistence to fluoroquinolones in *Escherichia coli*. *PLoS Genet.* **5,** e1000760 (2009).

44. Ennis, D. G., Amunsden, S. K. & Smith, G. R. Genetic functions promoting homologous recombination in *Escherichia coli*: A study of inversions in phage λ. *Genetics* **115,** 11–24 (1987).

45. Gleckman, R., Blagg, N. & Joubert, D. W. Trimethoprim: Mechanisms of action, antimicrobial activity, bacterial resistance, pharmacokinetics, adverse reactions, and therapeutic indications. *Pharmacotherapy* **1,** 14–19 (1981).

46. Lewin, C. S. & T, S. J. DNA breakdown by the 4-quinolones and its significance. *J. Med Microbiol* **31,** 65–70 (2018).

47. Huang, L. C., Wood, E. A. & Cox, M. M. Convenient and reversible site-specific targeting of exogenous DNA into a bacterial chromosome by use of the FLP recombinase: The FLIRT system. *J. Bacteriol.* **179,** 6076–6083 (1997).

48. Frank, E. G., Hauser, J., Levine, A. S. & Woodgate, R. Targeting the UmuD, UmuD', and MucA' mutagenesis proteins to DNA by RecA protein. *Proc. Natl. Acad. Sci. U. S. A.* **90,** 8169–8173 (1993).

49. Blattner, F. R. *et al.* The complete genome sequence of *Escherichia coli* K-12. *Science.* **277,** 1453–1474 (1997).

50. Ho, C., Kulaeva, O. I., Levine, A. S. & Woodgate, R. A rapid method for cloning mutagenic DNA repair genes: Isolation of *umu*-complementing genes from multidrug resistance plasmids R391, R446b, and R471a. *J. Bacteriol.* **175,** 5411–5419 (1993).

51. Rangarajan, S., Woodgate, R. & Goodman, M. F. Replication restart in UV-irradiated Escherichia coli involving pols II, III, V, PriA, RecA and RecFOR proteins. *Mol. Microbiol.* **43,** 617–628 (2002).

52. Schneider, C. A., Rasband, W. S. & Eliceiri, K. W. NIH Image to ImageJ: 25 years of image analysis. *Nat. Methods* **9,** 671–675 (2012).

53. Sliusarenko, O., Heinritz, J., Emonet, T. & Jacobs-Wagner, C. High-throughput, subpixel-precision analysis of bacterial morphogenesis and intracellular spatio-temporal dynamics. *Mol. Microbiol.* **80,** 612–627 (2012).

Acknowledgements

MMC was supported by grant GM32335 from the National Institute of General Medical Sciences USA. RW was supported by funds from the National Institutes of Health, National Institute of Child Health and Human Development Intramural Research Program. AvO was supported by a Laureate Fellowship FL140100027 from the Australian Research Council.

Figure captions

Figure 1. Effects of ciprofloxacin and trimethoprim on live cells.

a, Ciprofloxacin inhibits DNA gyrase and forms a gyrase-stabilised cleavage complex which might inhibit replication forming single-stranded gaps. **b**, In addition, ciprofloxacin treatment leads to the accumulation of reactive oxygen species (ROS). ROS oxidise the nucleotide pool; pol IV can incorporate 8-oxo-dGTP. Following base-excision repair (BER), single-stranded gaps (ssDNA) are created. The excision of closely spaced oxidised nucleotides leads to the formation of double-strand breaks (DSB). Following trimethoprim treatment, replication is inhibited which creates single-stranded regions. Similar to ciprofloxacin treatment, trimethoprim treatment interferes with the cellular metabolism and leads to ROS accumulation. Overall, ROS frequently convert single-stranded regions into DSBs. Ultimately, DNA breakage triggers the upregulation of pol IV, consequently, potentiating the effect of ROS within cells.

Figure 2. Pol IV concentration and activity following ciprofloxacin or trimethoprim treatment under oxidised or radical-scavenging conditions

a, Fluorescence images showing cells expressing DinB-YPet (Pol IV) at 0, 90 and 180 min (left to right) after ciprofloxacin-alone, ciprofloxacin-DMSO, trimethoprim-alone or trimethoprim-DMSO treatment (top to bottom). Scale bar represents 5 μm. **b**, Concentration of DinB-YPet during stress. Mean cell brightness is plotted against time (ciprofloxacin-alone: dark grey line, ciprofloxacin-DMSO: light grey line, trimethoprim-alone: magenta line, trimethoprim-DMSO: light magenta line). At each time-point, data are derived from >100 cells. Error bars represent standard error of the mean. **c**, Number of DinB-YPet foci per cell are plotted against time (ciprofloxacin-alone: dark grey line, ciprofloxacin-DMSO: light grey line, trimethoprim-alone: magenta line, trimethoprim-DMSO: light magenta line). At each time-point, data are derived from >100 cells. Error bars represent standard error of the mean.

Figure 3. SulA expression levels following ciprofloxacin or trimethoprim treatment under oxidised or radical-scavenging conditions in different genetic backgrounds

a, Fluorescence images showing the expression of GFP from a SOS reporter plasmid (P*sulA*-GFP) at 0, 60, 120 and 180 min (left to right) after ciprofloxacin-alone, ciprofloxacin-DMSO, ciprofloxacin-alone in Δ*recB*, trimethoprim-alone, trimethoprim-

DMSO or trimethoprim-BiP treatment (top to bottom). Scale bar represents 5 μm. **b**, SulA expression levels during stress. Mean cell brightness is plotted against time (ciprofloxacin-alone: dark grey line, ciprofloxacin-DMSO: light grey line, ciprofloxacin in Δ*recB*: purple, dotted line, trimethoprim-alone: magenta line, trimethoprim-DMSO: light magenta line, trimethoprim-BiP: rose-coloured, dashed line). Error bars represent standard error of the mean.

Figure 4. Number of pol IV foci per cell in *lexA*(Def) cells following ciprofloxacin or trimethoprim treatment under oxidised or radical-scavenging conditions

a, Upper row: Average projection in time (100 ms x 10 frames) showing DinB-YPet (pol IV) foci. Bottom row: Discoidal filtered projections. Cells were treated for 60 min prior to imaging. **b**, Number of DinB-YPet foci per cell. Error bars represent standard error of the mean. Number of cells included in analysis: *n*(ciprofloxacin) = 106, *n*(ciprofloxacin-DMSO) = 109, *n*(ciprofloxacin in Δ*recB*) = 106, *n*(trimethoprim) = 145, *n*(trimethoprim-DMSO) = 102, *n*(trimethoprim in Δ*recB*) = 94, *n*(untreated *recB*$^+$) = 85, *n*(untreated Δ*recB*) = 99.

Supplementary Figure 1. Characterising functionality of fluorescent fusion proteins.

a, Plate-based survival assays using ciprofloxacin or trimethoprim under oxidised or radical-scavenging conditions. Cell cultures (WT, *dnaX-mKate2*, *dinB-YPet*, *dinB-YPet dnaX-mKate2*, Δ*dinB*, *dnaX-YPet*, *umuC-mKate2*, *umuC-mKate2 dnaX-YPet* and Δ*umuDC*) were grown to exponential growth phase (OD_{600} = 0.2), serial diluted, and spotted onto LB agar plates +/- DMSO, plates containing 12 ng/mL ciprofloxacin +/- DMSO and plates containing 0.1 ng/mL trimethoprim +/- DMSO. Under antibiotic treatment, the addition of DMSO rescues survival by one to two orders of magnitude. Cell constructs used in this study (*dinB-YPet dnaX-mKate2* and *umuC-mKate2 dnaX-YPet*) exhibit a similar phenotype to WT. **b**, Trimethoprim survival assay. Cell cultures (WT, Δ*dinB*, Δ*umuDC*, *dinB-YPet dnaX-mKate2* and *umuC-mKate2 dnaX-YPet*) were grown to exponential growth phase (OD_{600} = 0.3). Then, trimethoprim was added to 1 μg/mL. At each time point (0, 0.5, 1, 2, 3 and 5 h), 500 μL culture was taken, twice centrifuged and resuspended in 500 μL LB. Finally, 50 μL were plated on LB agar plates; three technical replicates were made. Plates were incubated at 37^0C in the dark. Colonies were counted and CFU/mL were calculated for each time point as an average over the technical replicates. Error bars represent standard error of the mean over two biological replicates.

Supplementary Figure 2. Plate-based survival assays using ciprofloxacin or trimethoprim under oxidised or radical-scavenging conditions.

a, Strains (WT, Δ*dinB* and Δ*umuDC*) were grown to exponential growth phase (OD_{600} = 0.2), serial diluted, and spotted onto LB agar plates containing no antibiotic (LB), 12 ng/mL of ciprofloxacin or 12 ng/mL of ciprofloxacin plus 2% v/v DMSO. The addition of DMSO rescues survival by two orders of magnitude relatively to ciprofloxacin treatment. **b**, Replicate of **a**. **c**, Strains (WT, Δ*dinB* and Δ*umuDC*) were grown to exponential growth phase (OD_{600} = 0.2), serial diluted, and spotted onto LB agar plates containing no antibiotic (LB), 0.1 μg/mL of trimethoprim or 0.1 μg/mL of trimethoprim plus 2% v/v DMSO. The addition of DMSO rescues survival by two orders of magnitude relatively to ciprofloxacin treatment. Cells lacking *dinB* also have increased survival upon trimethoprim treatment. **d**, Strains (WT, Δ*dinB* and Δ*umuDC*)

were grown to exponential growth phase (OD_{600} = 0.2), serial diluted, and spotted onto LB agar plates containing no antibiotic (LB), 0.2 μg/mL of trimethoprim or 0.2 μg/mL of trimethoprim plus 2% v/v DMSO. The addition of DMSO rescues survival by two to three orders of magnitude relatively to ciprofloxacin treatment. Deleting *dinB* also increases survival upon trimethoprim treatment.

Supplementary Figure 3. Scatter plots of cell-size from time-lapse imaging. White points indicate individual data-points, while blue-to-red contours indicate frequencies of observations. Blue areas indicate regions of the plot containing few data points; red areas indicate regions containing a large number of data points. Frequencies were normalised at each time-point to the maximum value at that time-point.

a, EAW643 cells (*dinB-YPet dnaX-mKate2*) treated with ciprofloxacin-alone. **b**, EAW643 cells (*dinB-YPet dnaX-mKate2*) treated with ciprofloxacin-DMSO. **c**, EAW643 cells (*dinB-YPet dnaX-mKate2*) treated with trimethoprim-alone. **d**, EAW643 cells (*dinB-YPet dnaX-mKate2*) treated with trimethoprim-DMSO. **e**, SSH091 cells (MG1655 P*sulA*-GFP) treated with ciprofloxacin-alone. **f**, SSH091 cells (MG1655 P*sulA*-GFP) treated with ciprofloxacin-DMSO. **g**, SSH091 cells (MG1655 P*sulA*-GFP) treated with trimethoprim-alone. **h**, SSH091 cells (MG1655 P*sulA*-GFP) treated with trimethoprim-DMSO. **i**, SSH091 cells (MG1655 P*sulA*-GFP) treated with trimethoprim-BiP. **j**, SSH111 cells (Δ*recB* P*sulA*-GFP) treated with ciprofloxacin. We conservatively estimate that >100 cells were used in each measurement.

Supplementary Figure 4. SulA expression levels following ciprofloxacin-alone treatment in ΔrecB vs. MG1655 (wild-type)

a, Fluorescence images showing the expression of GFP from a SOS reporter plasmid (P*sulA*-GFP) from 0-110 min at intervals of 10 min and 120 min after ciprofloxacin addition in Δ*recB*. Scale bar represents 5 μm. **b**, Fluorescence images showing the expression of GFP from a SOS reporter plasmid (P*sulA*-GFP) at 120 min after ciprofloxacin addition in wild-type cells, MG1655. Scale bar represents 5 μm.

Supplementary Figure 5. Measuring colocalisation of pol IV with replisomes following ciprofloxacin or trimethoprim treatment under oxidised or radical-scavenging conditions

a, Merged images showing DinB-YPet (pol IV) foci in green and DnaX-mKate2 (replisome) foci in magenta at 0, 90 and 180 min (left to right) for ciprofloxacin-alone or ciprofloxacin-DMSO treatment (top to bottom). White arrows indicate colocalization events (white foci). Scale bar represents 5 μm. **b**, Merged images showing DinB-YPet (pol IV) foci in green and DnaX-mKate2 (replisome) foci in magenta at 0, 90 and 180 min (left to right) for trimethoprim-alone or trimethoprim-DMSO treatment (top to bottom). White arrows indicate colocalization events (white foci). Scale bar represents 5 μm. **c**, Colocalisation measurements following ciprofloxacin-alone treatment over 180 min: percentage of pol IV foci that are bound at replisomes (green line), percentage of replisomes that contain a pol IV focus (magenta line). Error bars represent the standard error of the mean from six biological replicates together. Measurements are from >300 cells per time point. **d**, Colocalisation measurements following ciprofloxacin-DMSO treatment over 180 min: percentage of pol IV foci that are bound at replisomes (green line), percentage of replisomes that contain a pol IV

focus (magenta line). Error bars represent the standard error of the mean from four biological replicates together. Measurements are from >100 cells per time point. **e**, Colocalisation measurements following trimethoprim-alone treatment over 180 min: percentage of pol IV foci that are bound at replisomes (green line), percentage of replisomes that contain a pol IV focus (magenta line). Error bars represent the standard error of the mean from three biological replicates together. Measurements are from >100 cells per time point. **f**, Colocalisation measurements following trimethoprim-DMSO treatment over 180 min: percentage of pol IV foci that are bound at replisomes (green line), percentage of replisomes that contain a pol IV focus (magenta line). Error bars represent the standard error of the mean from three biological replicates together. Measurements are from >100 cells per time point.

Supplementary Figure 6. Measuring the colocalisation of pol IV and replisomes following ciprofloxacin or trimethoprim treatment under oxidised or radical-scavenging conditions in *lexA*(Def) cells

a, DinB-YPet activity at replisomes in *lexA*(Def) cells. Cells were treated for 60 min prior to imaging. Merged images showing DinB-YPet foci in green and DnaX-mKate2 foci in magenta following ciprofloxacin-alone, ciprofloxacin-DMSO, trimethoprim-alone and trimethoprim-DMSO treatment (from left to right). White arrow points at colocalisation event (white focus). Scale bar represents 5 μm. **b**, Colocalisation percentages of pol IV foci that bind at replisomes (green bars) and colocalisation percentages of replisomes that contain a pol IV focus (magenta bars) for cells treated with ciprofloxacin-alone (left) or ciprofloxacin-DMSO (right). Colocalisation was measured with sets of pol IV foci that last 1, 3, 5 and 10 s. Error bars represent the standard error of the mean. **c**, Colocalisation percentages of pol IV foci that bind at replisomes (green bars) and colocalisation percentages of replisomes that contain a pol IV focus (magenta bars) for cells treated with trimethoprim-alone (left) or trimehtoprim-DMSO (right). Colocalisation was measured with sets of pol IV foci that last 1, 3, 5 and 10 s. Error bars represent the standard error of the mean.

Supplementary Figure 7. Measuring the number of pol V foci per cell following ciprofloxacin or trimethoprim treatment under oxidised or radical-scavenging conditions in *lexA*(Def) cells

a, UmuC-mKate2 activity at replisomes in *lexA*(Def) cells. Cells were treated for 60 min prior to imaging. Upper row: unfiltered image of an average projection showing UmuC-mKate2 foci that last >1s (from left to right: ciprofloxacin, ciprofloxacin-DMSO, trimethoprim, trimethoprim-DMSO). Bottom row: merged image showing UmuC-mKate2 foci in magenta and DnaX-YPet foci in green (from left to right: ciprofloxacin, ciprofloxacin-DMSO, trimethoprim, trimethoprim-DMSO). Scale bar represents 5 μm. **b**, Number of UmuC-mKate2 foci per cell. Error bars represent standard error of the mean. Number of cells included in analysis: *n*(ciprofloxacin) = 97, *n*(ciprofloxacin-DMSO) = 109, *n*(untreated) = 87. **c**, Binding behaviour of UmuC-mKate2 at replisomes after ciprofloxacin-alone or ciprofloxacin-DMSO treatment. Mean average autocorrelation function (ciprofloxacin-alone: dark grey line, ciprofloxacin-DMSO: light grey line). Error bar represents standard error of the mean. We conservatively estimate that >400 trajectories from >400 replisomes were used in each measurement. **d**, Number of UmuC-mKate2 foci per cell. Error bars represent standard error of the mean. Number of cells included in analysis: *n*(trimethoprim) =

102, *n*(trimethoprim-DMSO) = 120, *n*(untreated) = 87. **e**, Binding behaviour of UmuC-mKate2 at replisomes after trimethoprim-alone or trimethoprim-DMSO treatment. Mean average autocorrelation function (trimethoprim-alone: magenta line, trimethoprim-DMSO: light magenta line). Error bar represents standard error of the mean. We conservatively estimate that >550 trajectories from >550 replisomes were used in each measurement.

Supplementary Figure 8. UmuC concentration and activity following ciprofloxacin or trimethoprim treatment under oxidised or radical-scavenging conditions

a, Images showing UmuC-mKate2 (pol V) signal at 0, 90 and 180 min (left to right) for ciprofloxacin-alone, ciprofloxacin-DMSO treatment or trimethoprim-alone treatment (top to bottom). Scale bar represents 5 µm. **b**, Merged images showing UmuC-mKate2 (pol V) foci in magenta and DnaX-YPet (replisome) foci in magenta at 0, 90 and 180 min (left to right). Colocalised foci would appear as white foci. Scale bar represents 5 µm. **c**, Concentration of UmuC-mKate2 during stress. Mean cell brightness is plotted against time (ciprofloxacin-alone: dark grey line, ciprofloxacin-DMSO: light grey line, trimethoprim-alone: magenta line). At each time-point, data are derived from >100 cells. Error bars represent standard error of the mean. **d**, Colocalisation measurements following ciprofloxacin-alone treatment over 180 min: percentage of UmuC foci that are bound at replisomes (magenta line), percentage of replisomes that contain a UmuC focus (green line). Error bars represent the standard error of the mean from three biological replicates together. Measurements are from >100 cells per time point. **e**, Colocalisation measurements following ciprofloxacin-DMSO treatment over 180 min: percentage of UmuC foci that are bound at replisomes (magenta line), percentage of replisomes that contain a UmuC focus (green line). Error bars represent the standard error of the mean from three biological replicates together. Measurements are from >100 cells per time point.

Supplementary Figure 9. Western blots with anti-UmuD antibodies measuring levels of UmuD'. For each lane, 30 µL of lysate were loaded from cultures at OD_{600} 0.5. All strains used are Δ*umuDC* expressing UmuDC from a low-copy number plasmid (pRW154). After treatment, time points were taken at 1, 2, 3h. Rabbit anti-UmuD antibody 1:

a, Western blot of *recA*$^+$ *lexA*$^+$ cells (RW120): untreated, treated with ciprofloxacin or ciprofloxacin + 2% DMSO. **b**, Western blot of *recA*$^+$ *lexA*$^+$ cells: untreated, treated with trimethoprim or trimethoprim + 2% DMSO. **c**, Western blot of *recA*$^+$ *lexA51*(Def) cells (RW546): untreated, treated with ciprofloxacin or ciprofloxacin + 2% DMSO. **d**, Western blot of *recA*$^+$ *lexA51*(Def) cells: untreated, treated with trimethoprim or trimethoprim + 2% DMSO.

Supplementary Movie 1. Time-lapse movie of Δ*recB* cells carrying P*sulA*-GFP. Ciprofloxacin (30 ng/mL) was added to the media ay t = 0 min. An image was taken every 10 min over the period of 3 h. Upper movie: bright-field, bottom movie: signal from GFP expression (level of SOS induction).

Supplementary Movie 2. Burst acquisition movies of DinB-YPet in *recB*$^+$ cells treated with 1 µg/mL trimethoprim (TMP, ± DMSO) or 30 ng/mL ciprofloxacin (± DMSO), Δ*recB* cells treated with TMP or ciprofloxacin. Movies were recorded 60 min after antibiotic addition. Frames were taken every 0.1 s.

Figure 1

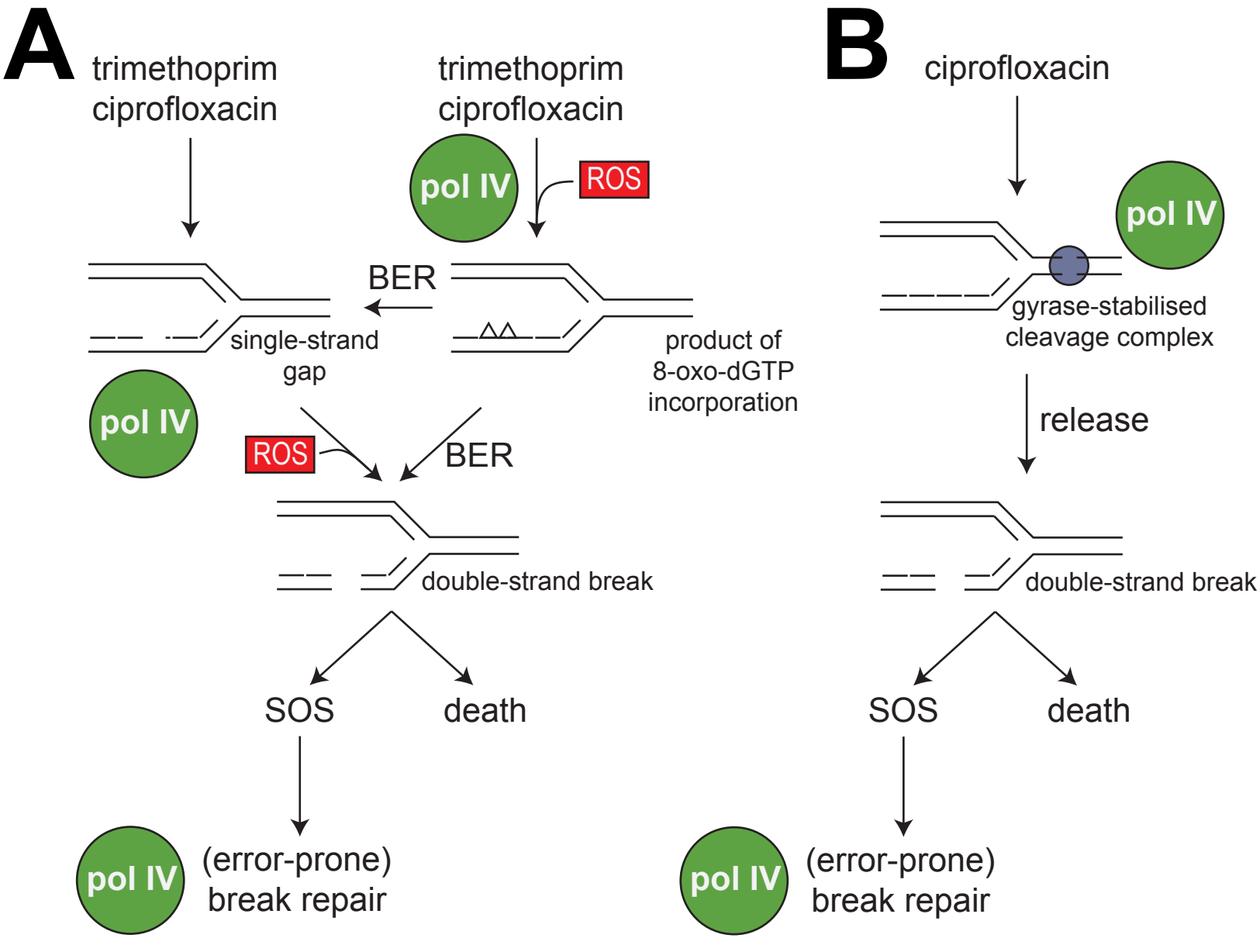
A
trimethoprim
ciprofloxacin
trimethoprim
ciprofloxacin
pol IV
ROS
BER
single-strand
gap
product of
8-oxo-dGTP
incorporation
pol IV
ROS
BER
double-strand break
SOS
death
pol IV
(error-prone)
break repair
B
ciprofloxacin
pol IV
gyrase-stabilised
cleavage complex
release
double-strand break
SOS
death
pol IV
(error-prone)
break repair

Figure 2

A Fluorescence images: Signal DinB-YPet (Pol IV):

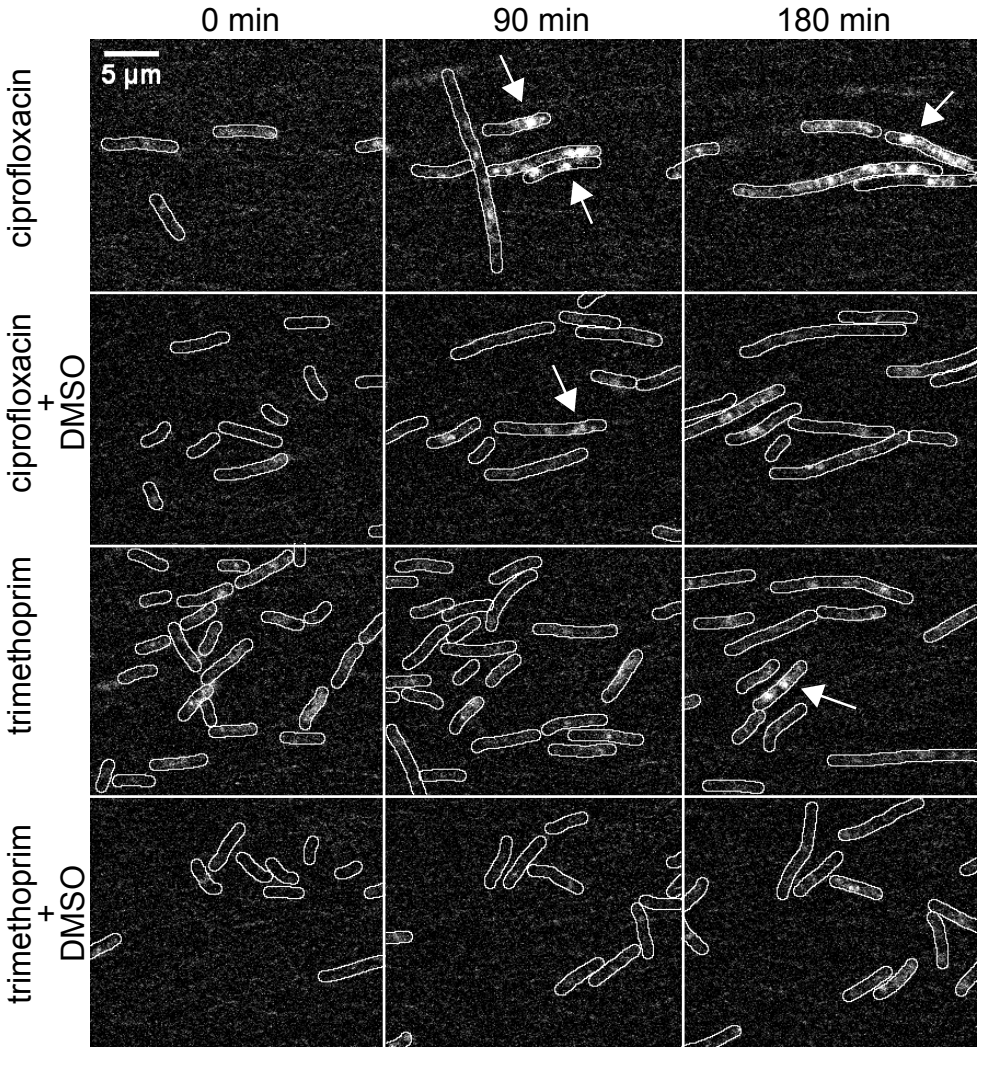

B DinB-YPet concentration

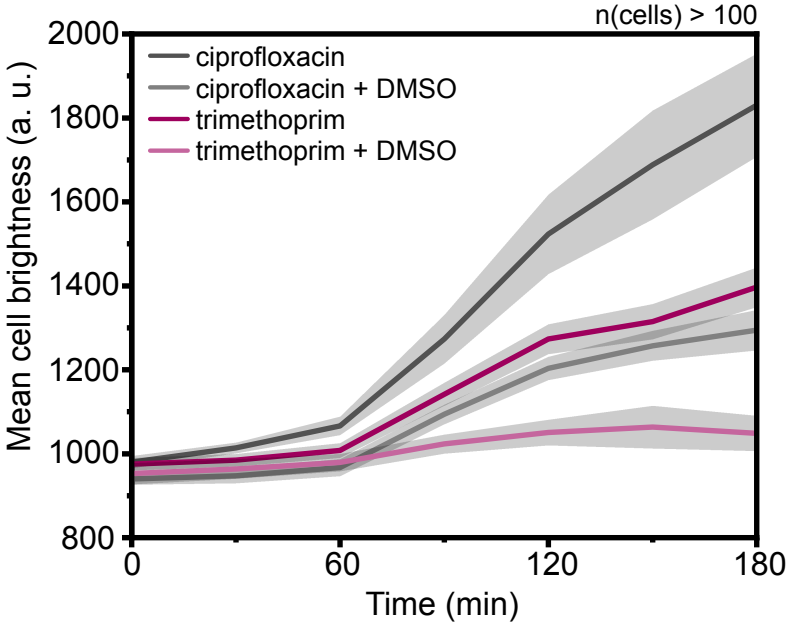

C DinB-YPet activity: focus formation

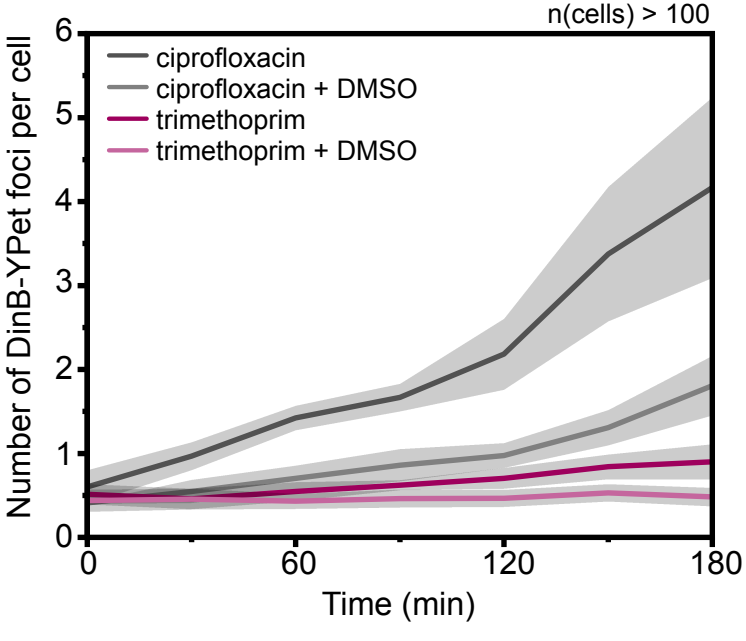

Figure 3

A **Fluorescence images: SOS reporter plasmid (P*sulA*-GFP):**

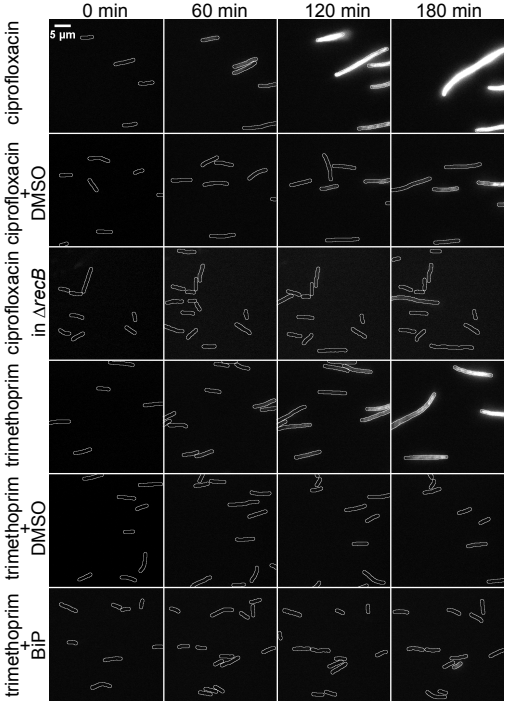

B **SulA expression levels: oxygen scavangers inhibit SOS induction**

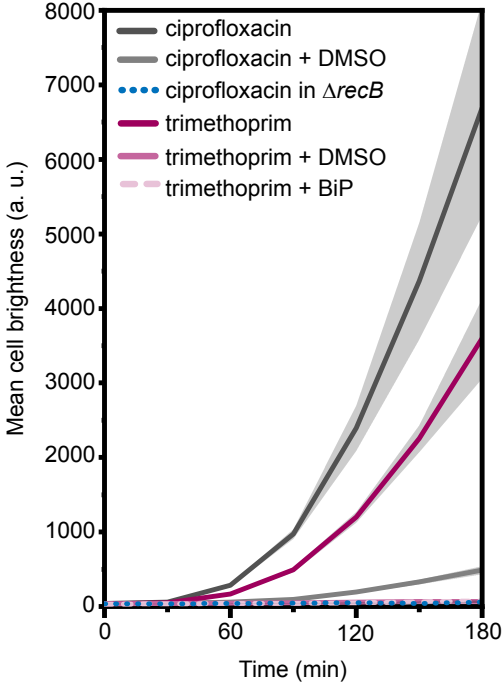

Figure 4

A DinB-YPet activity in *lexA(Def)*

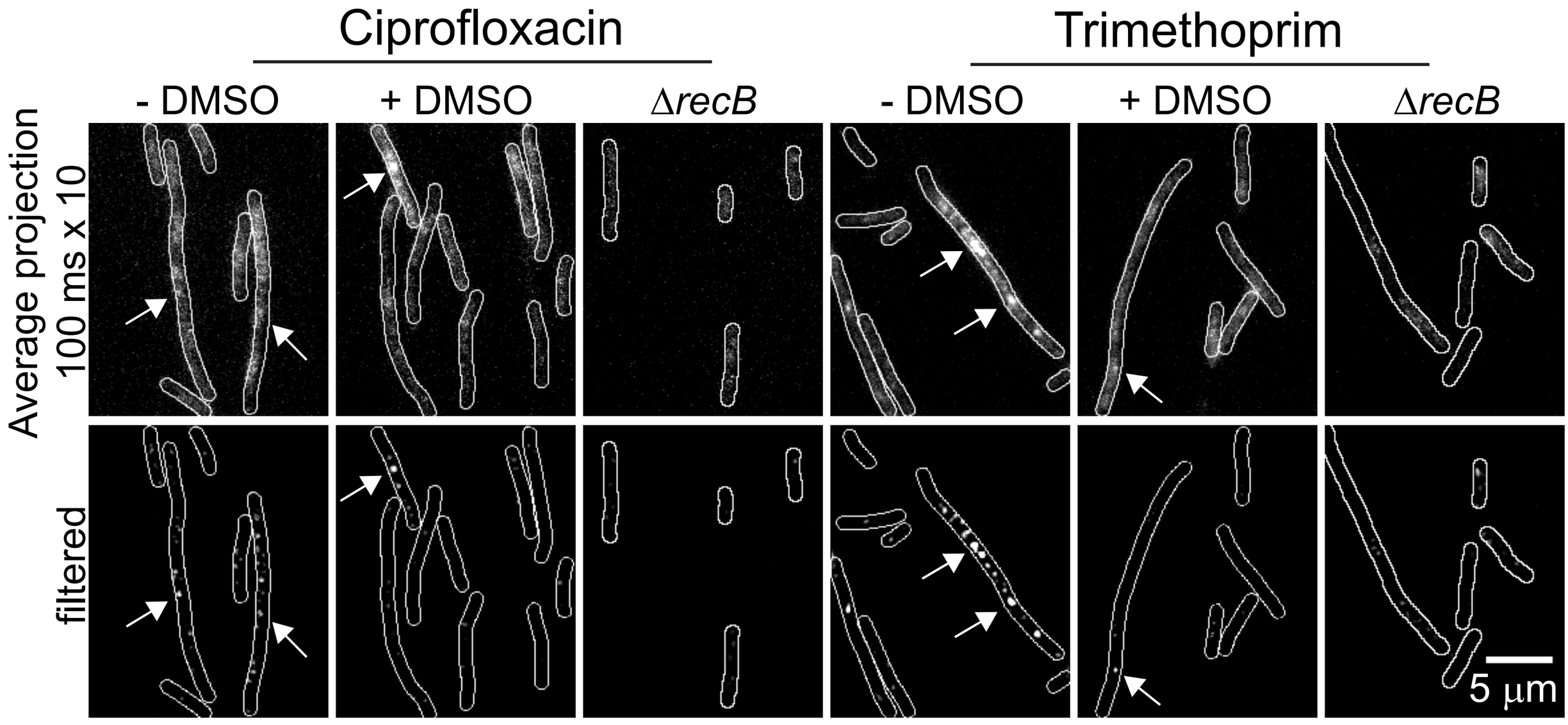

B Mean DinB foci per cell

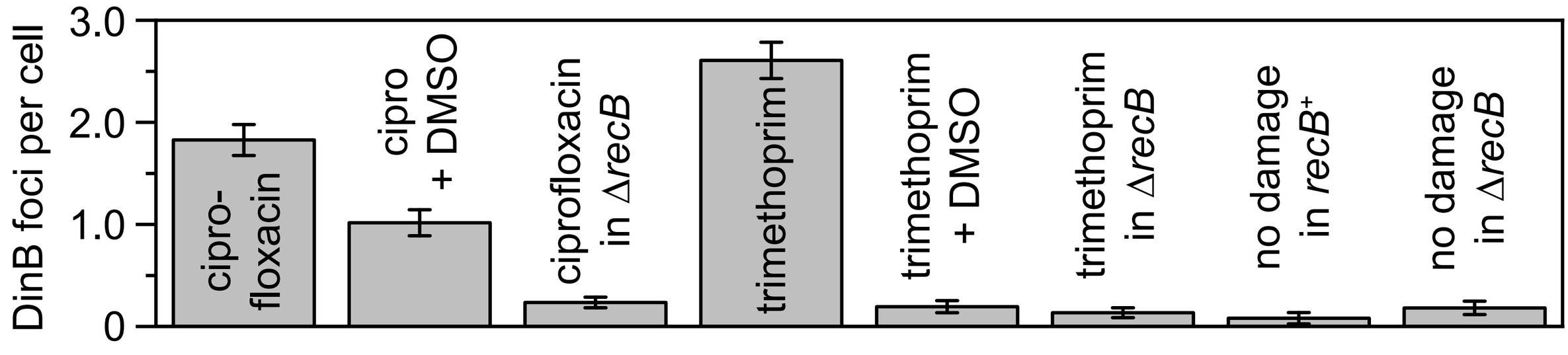

Supplementary Figure 1

A Plate-based survival assay

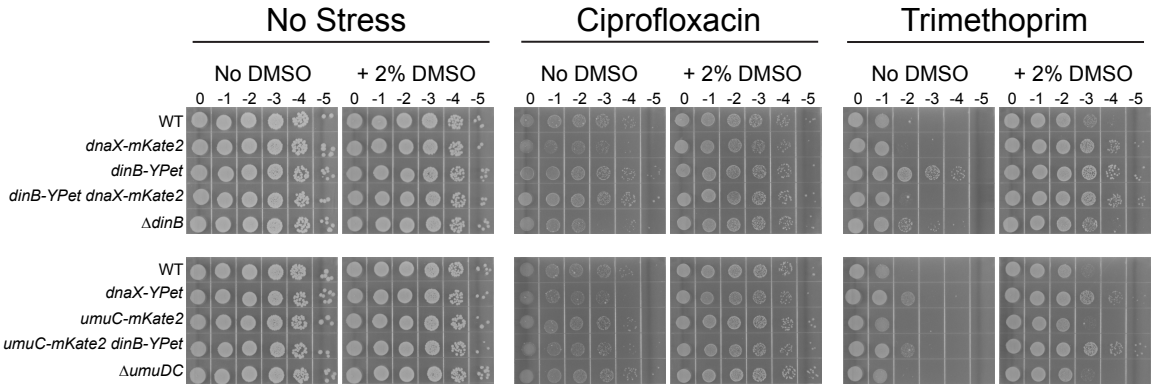

B Survival assay over time

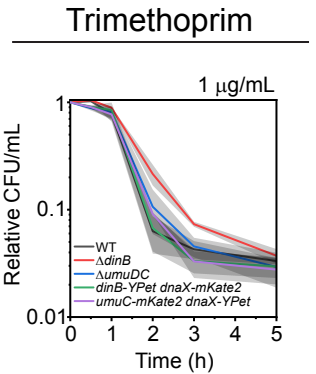

Supplementary Figure 2

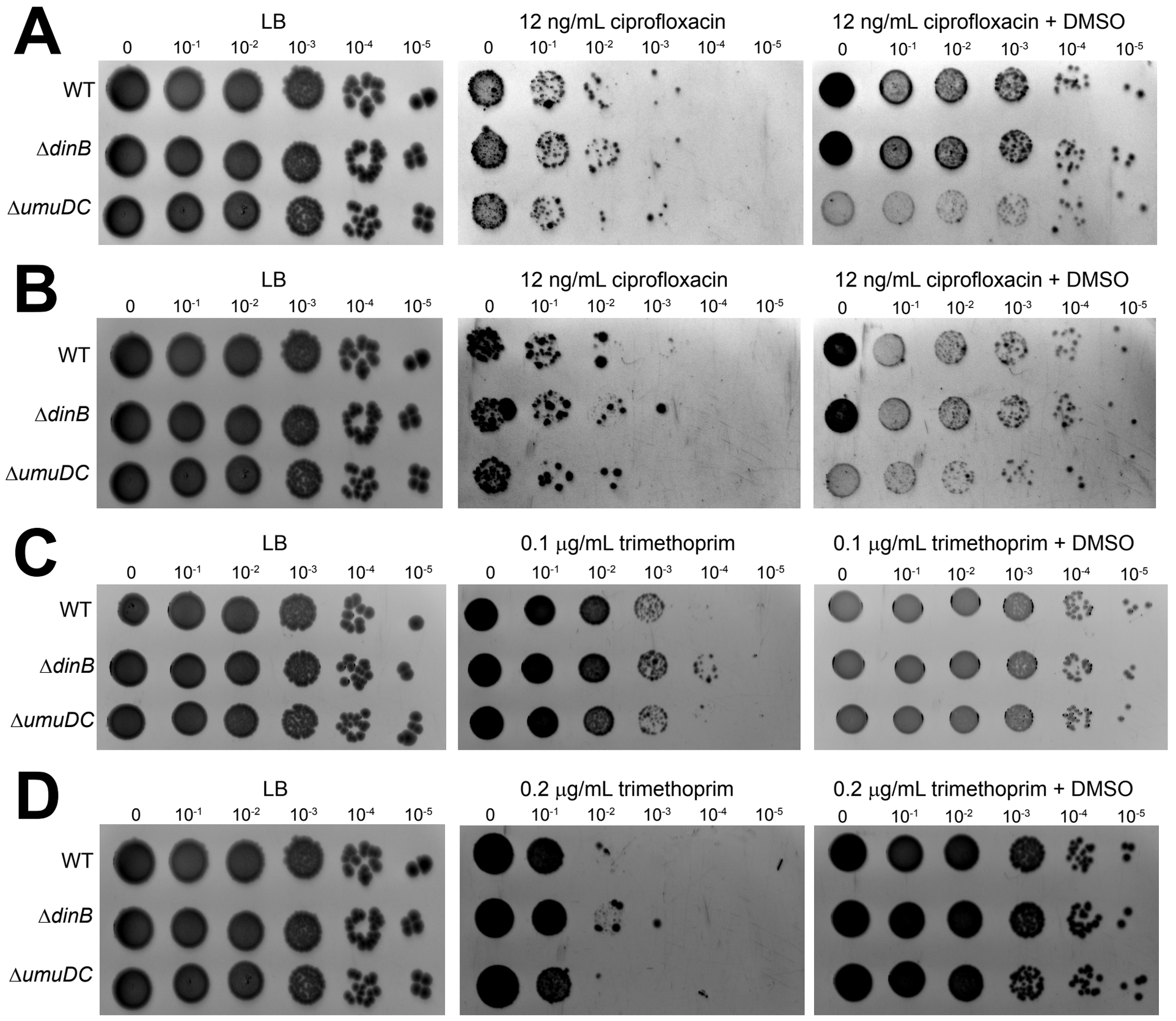

Supplementary Figure 3

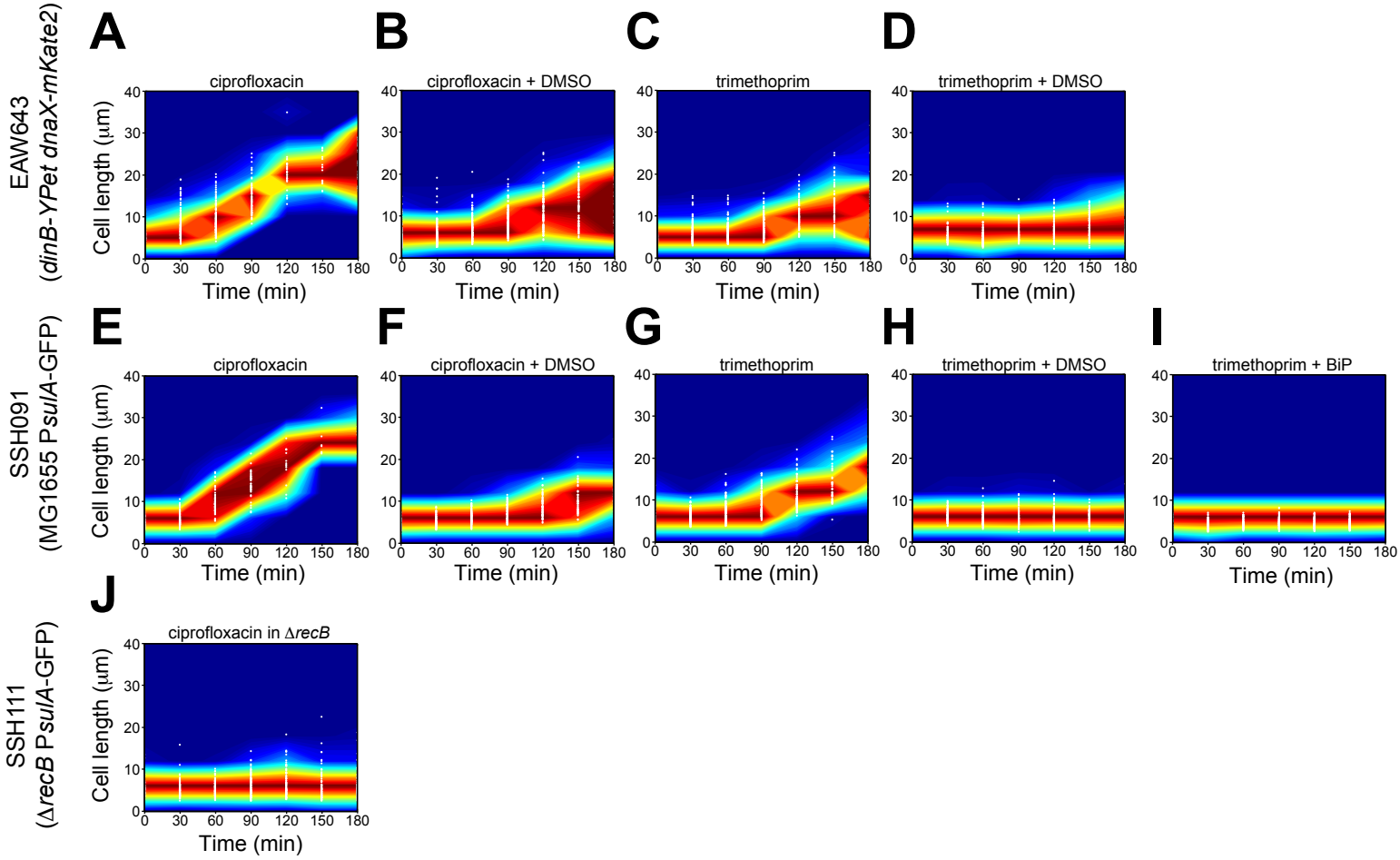

Supplementary Figure 4

A **Fluorescence images following ciprofloxacin treatment: SOS reporter plasmid (P*sulA*-GFP) in Δ*recB***

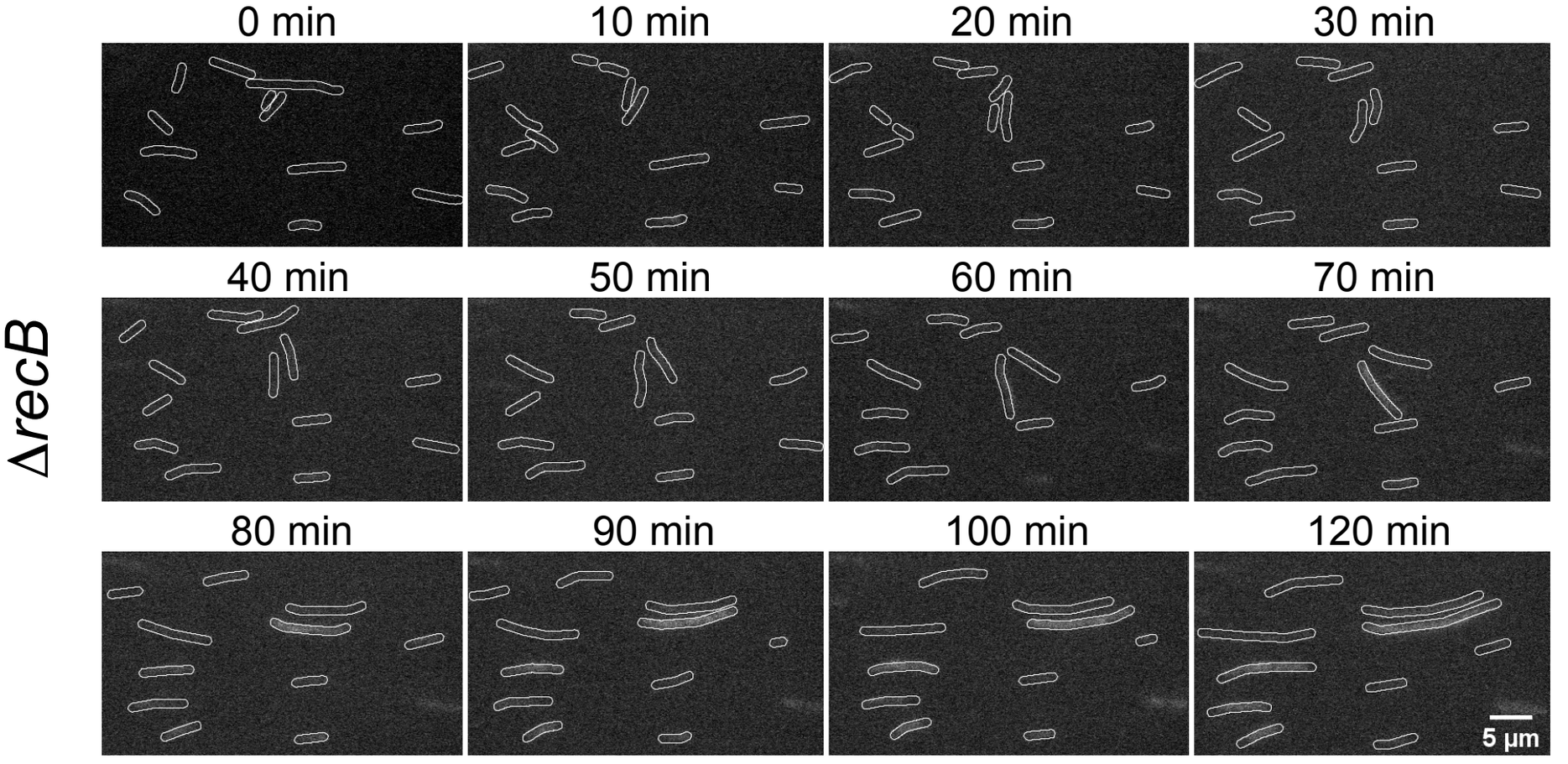

B **Fluorescence image following ciprofloxacin treatment: SOS reporter plasmid (P*sulA*-GFP) in MG1655**

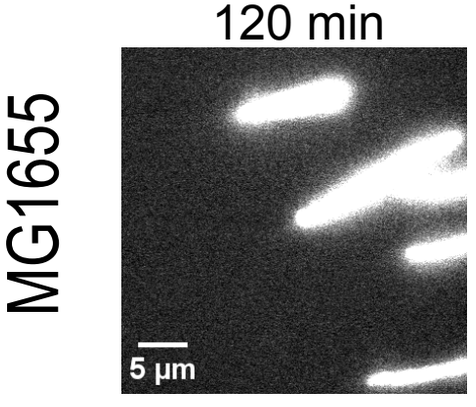

Supplementary Figure 5

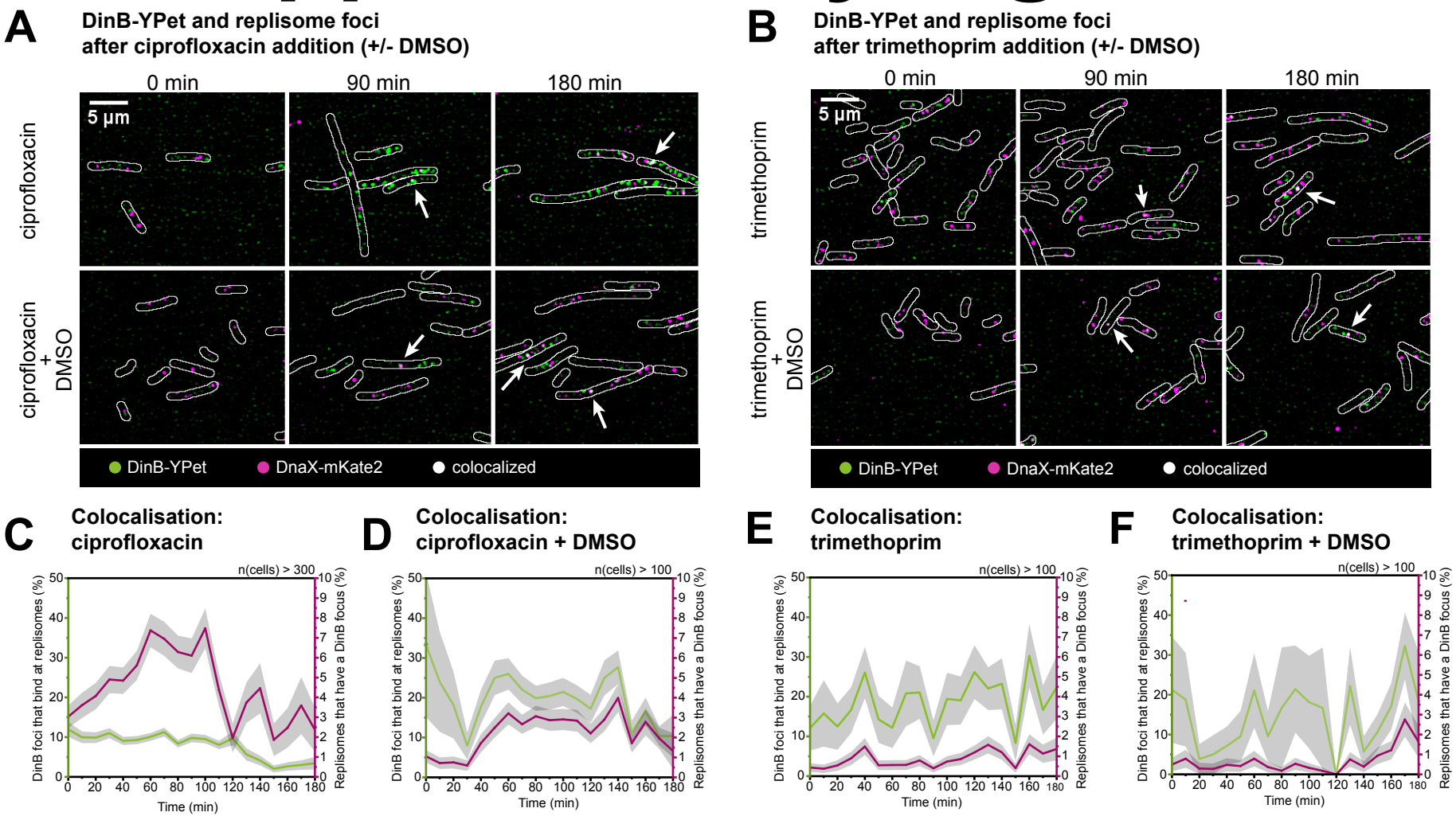

Supplementary Figure 6

A **Merged images: DinB-YPet (pol IV) activity at replisomes**

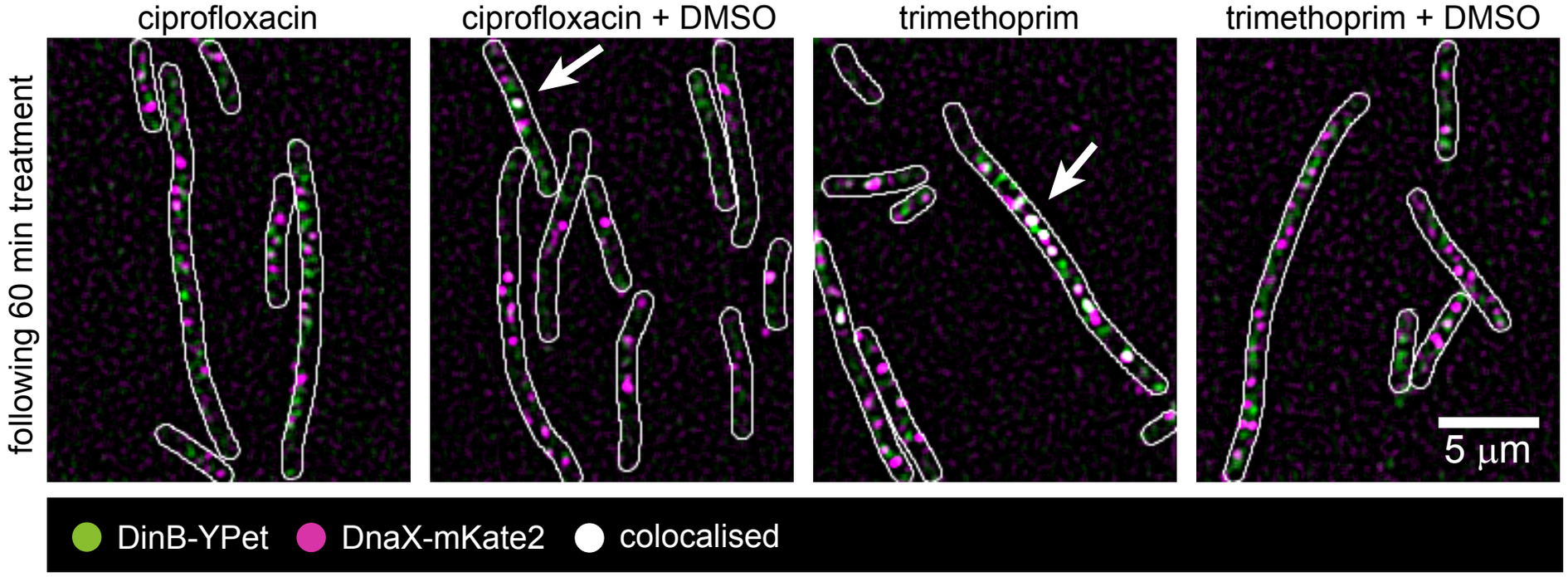

B **Colocalisation: ciprofloxacin (+/- DMSO)**

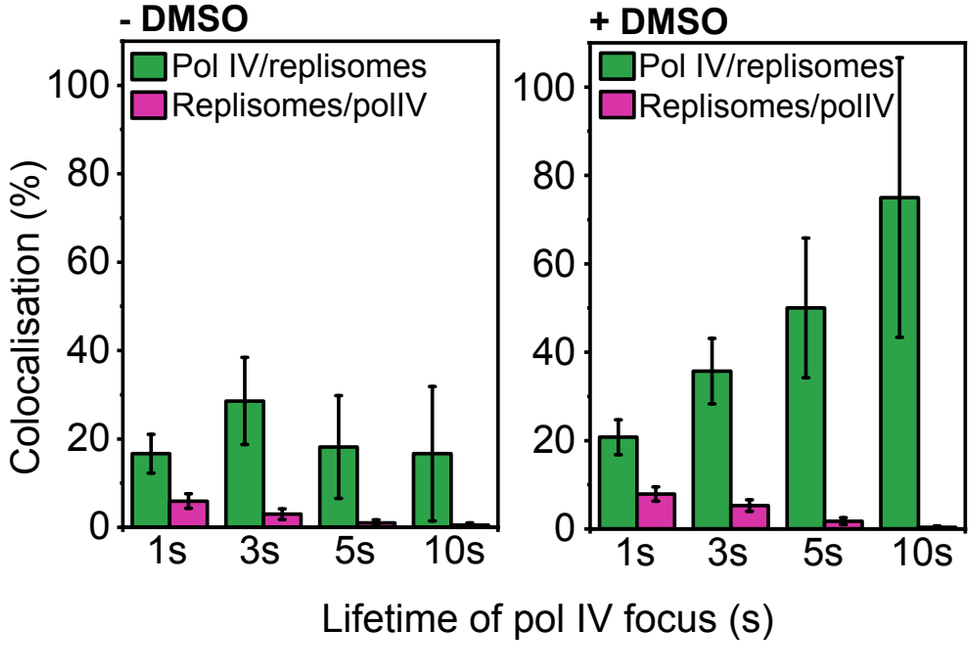

C **Colocalisation: trimethoprim (+/- DMSO)**

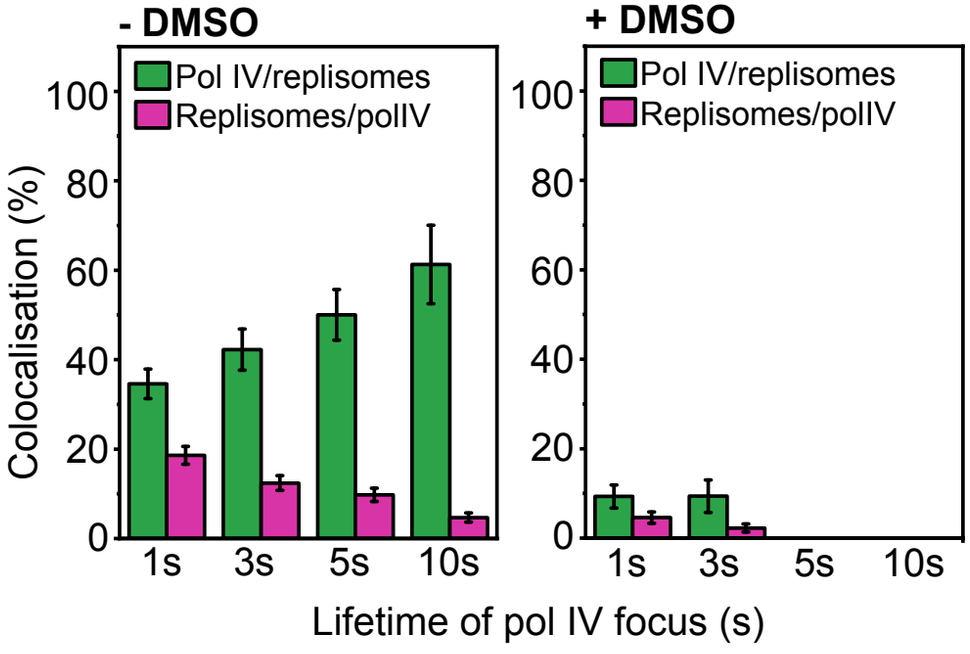

Supplementary Figure 7

A **UmuC-mKate2 (pol V) activity at replisomes**

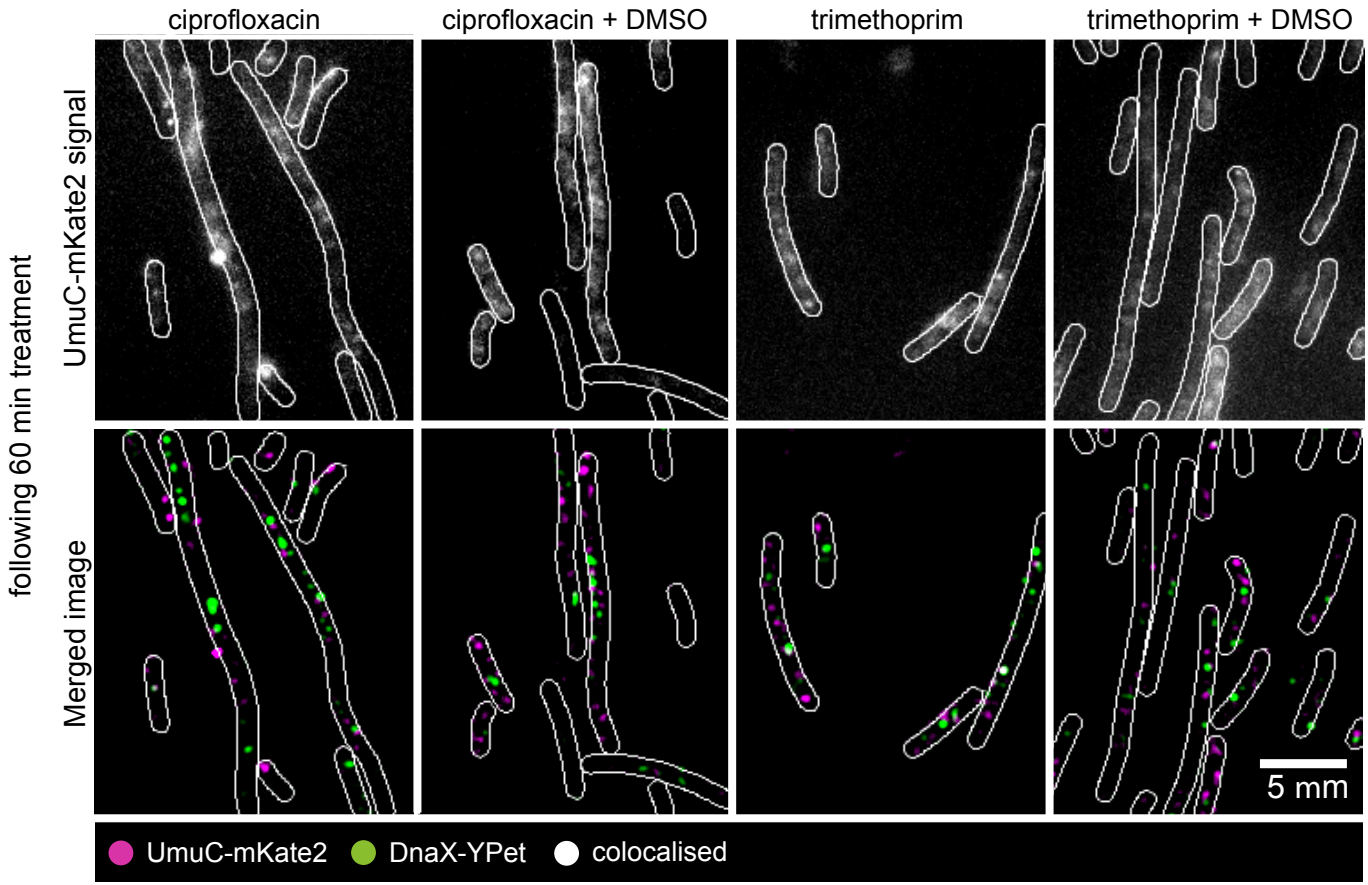

B **Number of UmuC foci per cell: ciprofloxacin (+/- DMSO)**

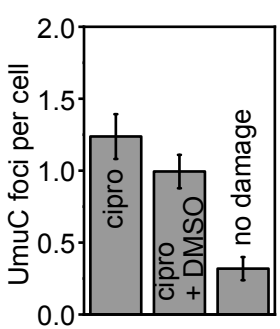

C **Number of UmuC foci per cell: trimethoprim (+/- DMSO)**

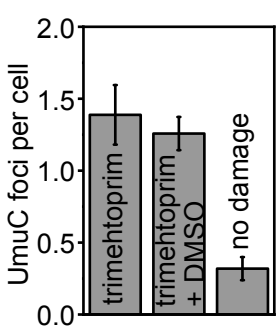

Supplementary Figure 8

A **Fluorescence images: Signal UmuC-mKate2 (Pol V):**

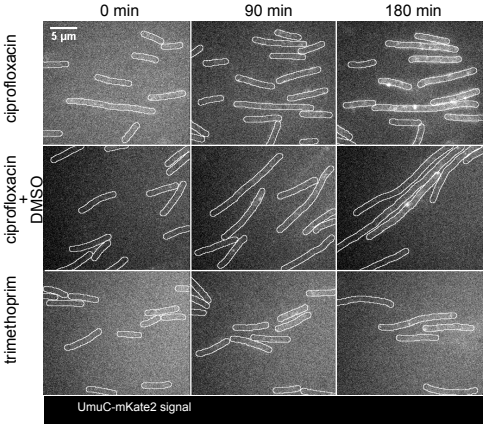

B **UmuC-mKate2 and replisome foci during stress**

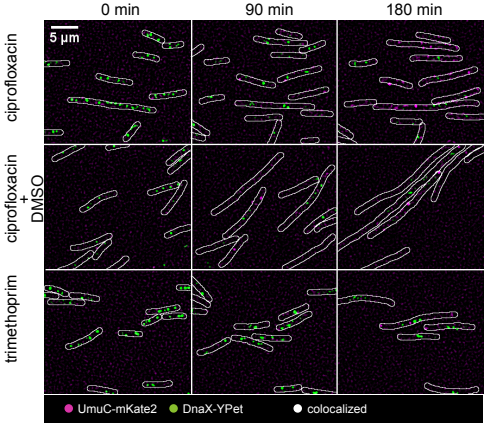

C **UmuC-mKate2 concentration during stress**

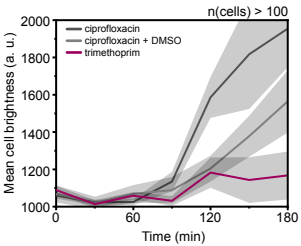

D **Colocalisation: ciprofloxacin**

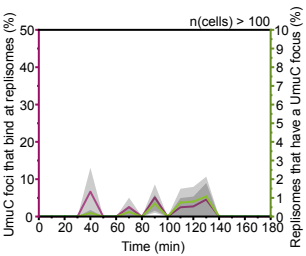

E **Colocalisation: ciprofloxacin + DMSO**

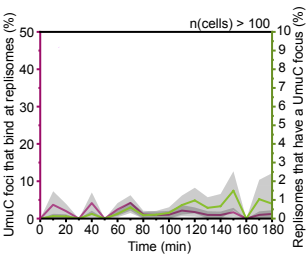

Supplementary Figure 9

A **Anti-UmuD Western blots for *recA*⁺ *lexA*⁺: ciprofloxacin**

chromosome: Δ*umuDC*; plasmid: UmuDC

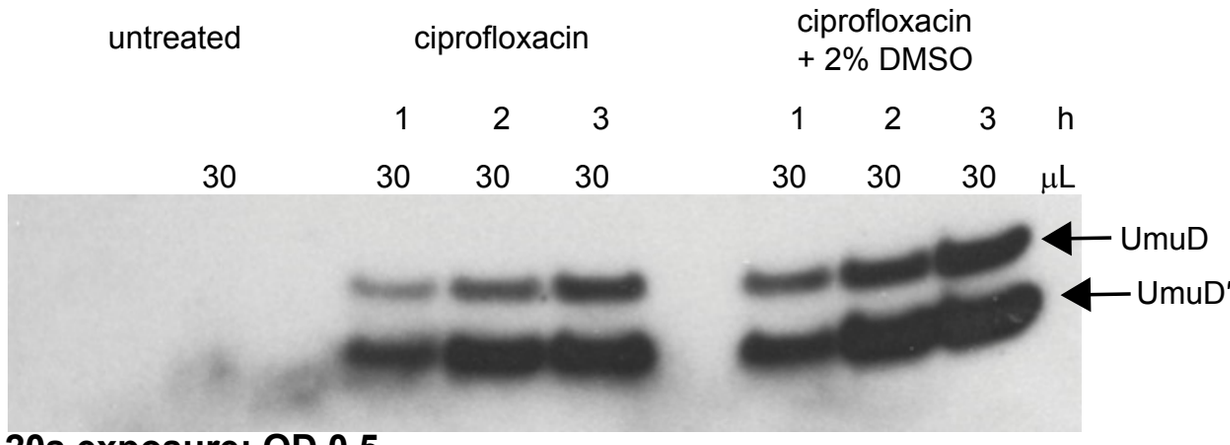

20s exposure; OD 0.5

B **Anti-UmuD Western blots for *recA*⁺ *lexA*⁺: trimethoprim**

chromosome: Δ*umuDC*; plasmid: UmuDC

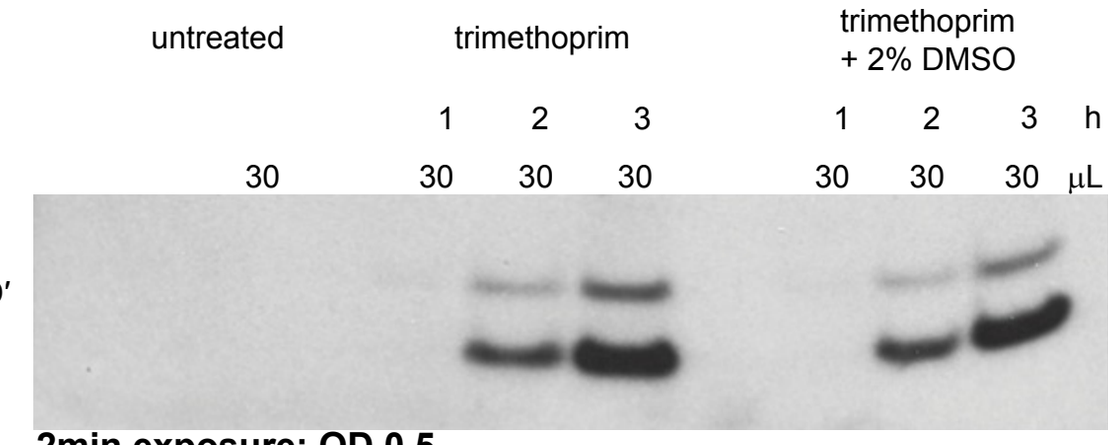

2min exposure; OD 0.5

C **Anti-UmuD Western blots for *recA*⁺ *lexA51*(Def): ciprofloxacin**

chromosome: Δ*umuDC*; plasmid: UmuDC

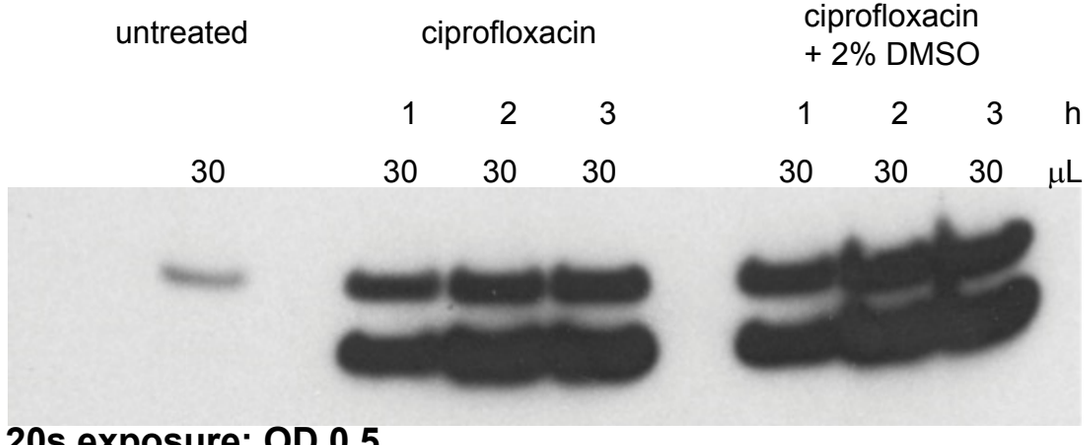

20s exposure; OD 0.5

D **Anti-UmuD Western blots for *recA*⁺ *lexA51*(Def): trimethoprim**

chromosome: Δ*umuDC*; plasmid: UmuDC

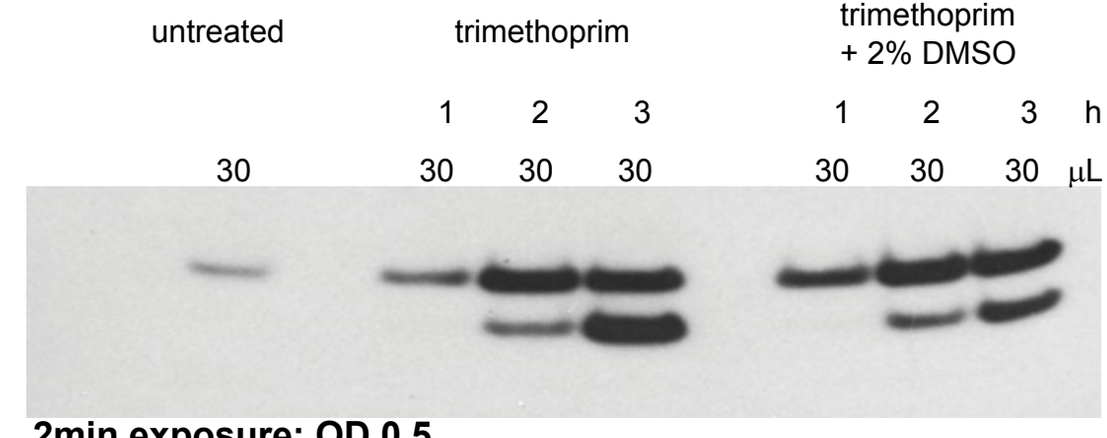

2min exposure; OD 0.5